Molecule−Metal Polarization at Rectifying GaAs Interfaces

Ayelet Vilan,† Jamal Ghabboun, and David Cahen*

Department of Materials & Interfaces, Weizmann Institute of Science, Rehovot, Israel 76100

Received: August 16, 2002; In Final Form: February 17, 2003

Metal/organic monolayer/GaAs junctions, prepared by adsorbing a set of dicarboxylic ligands, with systematic change of ligand substituents, on GaAs, are measured and characterized electrically. The molecules are chemically bound to the semiconductor surface under ambient conditions and form roughly a monolayer (MoL), with average order in the direction perpendicular to the semiconductor surface. This suffices to yield systematic changes in electron affinity and work function of the modified GaAs. Junctions are made by a soft metal deposition method, used here for Au and Al. Experimentally, we find strong molecular effects, reaching differences in current at a given voltage of up to 6 orders of magnitude, depending on the substituent on the molecules making up the monolayer. These and the changes in the effective barrier height of the metal/MoL/GaAs junctions, extracted by analyses of their current−voltage characteristics, can be explained by electrostatic effects of the molecular layer, rather than by electrodynamic ones (current flow through the molecular film). This can be understood by realizing that the samples are relatively large area devices with extremely narrow (∼1 nm) films of organic molecules, showing only average order, which makes dominance of tunneling effects very unlikely. We show that not only the molecule's electronic and electrical properties but also the way the metals contact the molecules, as well as the doping type of the semiconductor, can determine the direction of the molecular effect. Also the type of metal governs the effect that we identify as being due to interfacial dipoles formed as a result of triple metal/organic molecule/semiconductor interaction.

1. Introduction

Interest in electrical properties of single layers of molecules goes back almost 40 years.[1] In principle, these quasi-two-dimensional systems bear much resemblance to the quasi-one-dimensional (isolated) molecule systems, that, in "molecular electronics" are often viewed as potential (isolated) single molecule devices.[2] Their applicability to existing technology is, however, much larger.[3] During the 60s and 70s research on these systems focused on the insulating properties and charge-transfer mechanisms through thin molecular layers made either by the Langmuir−Blodgett (LB) method[4−7] or by self-assembly.[8] A major problem of these early studies was that the possible relation between molecular length and the quality of the layer was not considered. In other words, for this type of electrical investigation the density of "pinholes" (i.e., defects through the monolayer, with diameters up to several nm; cf. ref 9) must be well below chemical detection limits (i.e., lower than ppm).

One way to overcome the pinhole difficulty is by placing the top metal contact in a soft manner. As early as 1939, Race and Reynolds used a hanging mercury drop to measure the dielectric constant of Ba stearate multilayer LB films.[10] Later Mann and Kuhn used this (and other) method(s) to measure the conductivity of mono- and multilayer LB films of Cd salts of fatty acids. A Hg drop electrode was also used by Honig (who used stearic acid and Pb stearate layers), who found a strong dependence of the conductance on the electrode material. Honig noted that not all of this effect could be explained by the differences in metal work functions. He suggested that the electrode dictates the injection probability or the degree of charging of the interface.[6] Iwamoto and co-workers recently presented support for the latter explanation,[11] as they found highly asymmetric charge transfer from gold (Au) and aluminum (Al) into polyimide LB layers. The amount of charge transfer was calculated theoretically and measured experimentally and found to be dependent on the number of LB layers (from 1 to 99) as well as on the applied bias.[11] Lately Hg drops have been used also as substrates to study tunneling through the highly ordered self-assembled monolayers of alkanethiols and related molecules that can be formed on Hg.[12,13,15]

Enhanced electrical effects of the molecules can be achieved by using electrically active molecular constituents. Different combinations of molecular conductors and also donor−acceptor molecules were studied by Roth and co-workers.[16] They measured a tunneling current (at 4 K) through 1−3 stratified films of different molecules, with each of these made up of 1−10 molecular LB layers. The onset-bias of the current and further steps were clearly related to specific molecular energy levels.[16] Heath et al. made LB films of molecules with a voltage-dependent conformation. Inserting them in a "sandwich" configuration resulted in an electrochemical switch.[17,18] Selzer et al. used a series of cyclic disulfides, between Hg and Si to show strong negative differential resistance at room temperature, ascribed to voltage dependent poling of the monolayer.[61]

Understanding the electrical effects of molecules on solid *surfaces* is a necessary condition to elucidate the molecules' roles at *interfaces*. For modification of metals we can mention the change of Au work function by adsorption of an alkanethiol-based monolayer on its surface. As the dielectric constant of such a layer increases with the length of the alkyl chain, this results in a corresponding larger change in work function

* Corresponding author. E-mail: david.cahen@weizmann.ac.il. Phone: +972-8934-2246/3881. Fax: +972-8934-4138.

† Present address: Philips Research, 5656AA Eindhoven, The Netherlands.

10.1021/jp026779b CCC: $25.00
Published on Web 06/06/2003

because of the increasing potential drop over the layer of alkyl chains (see below, eq 8).[19,20] For semiconductors we can refer to a recent review on chemical modifications of compound semiconductors.[21] We found that organic molecules can bind chemically to a number of semiconductors via a carboxylate bond, with coverage of roughly one molecular layer (MoL[22]).[23−25] The MoL is partially organized with average orientation perpendicular to the surface. Thus, MoLs of benzoic acids with different substituent groups modify the effective electron affinity of GaAs by up to 1 eV, and adsorption of dicarboxylic ligands on CdTe modify both its electron affinity (by 0.8 eV) and its surface band bending (by 0.6 eV). Adsorbing the same dicarboxylic ligands on GaAs has a clear effect on the localized surface charge, something that we interpreted in terms of a change in the position (and density) of occupied surface states, depending also on the doping of the GaAs.[26] The direction of the dipole formed by adsorption of benzoic acids was found to be highly dependent on the interacting substrate atoms and could be inverted between ITO and Al.[27]

In terms of device applications, molecular layers were investigated with respect to their ability to modify the interfacial properties of (organic) optoelectronic devices to improve their net efficiency. Tredgold and co-workers studied the increase in efficiency of Au/GaP and /GaAs solar cells by introducing an LB polymeric layer at the cell's interface.[28,29] A change of up to 0.35 eV in potential barrier for transport (barrier height; vide infra) was measured depending on the density of carboxylic groups incorporated in the polymer. They also made Au/GaAs diodes with LB layers of stearic acids (thickness 2.4 nm) and perfluorodecanoic acids (thickness 1.7 nm) and found a similar effect on the barrier height. Therefore, they concluded that the surface density of dipoles is the major parameter rather than the insulator (alkyl chain) length.[30] The major role of interfacial electrostatics is being appreciated more and more in understanding Schottky barriers[31] and especially in the area of organic light emitting diodes (OLEDs).[32] Interactions of organic molecules and polymers with metals have been studied extensively by in situ UPS, XPS, and Kelvin probe measurements, following deposition of the molecules on the metal or vice versa[33] (for a review see ref 32). More recently Schlettwein et al. used a number of phthalocyanines to vary the molecular energy levels. They found a correlation between the molecular energies measured by UPS in the gas phase and the dipole of the molecular layer, deposited on the surface or the redistribution of charge at the interface region, depending on the ligand used.[34]

Adsorption of monolayers of small organic molecules is being explored also to modify the efficiency of OLEDs[35−38] and solar cells.[39,40] Much effort focused on modifying the hole injection properties of indium tin oxide (ITO), the most common transparent anode in OLEDs. Ganzorig et al. were able to modify the work function of ITO by up to 0.6 eV by varying either the binding group or the (para) substituent group of a series benzyl derivatives, adsorbed as MoL on the ITO. The corresponding change in current in an ITO/TPD/Al device, 3.5 decades (at +5V), drastically reduced the onset voltage for luminescence.[41] Nuesch et al. found ITO to be very sensitive also to inorganic chemical treatments (which were thought to leave a 1 nm thick layer of the corresponding salt on the surface). Immersion in dilute acid or base solution led to changes in the ITO work function by +0.7 and −0.6 eV, respectively, relative to a plasma-treated sample. These changes in work function affected the electroluminescence characteristics of TPD/Alq devices.[42]

Many of the above-mentioned molecularly modified devices were made by spin coating or vacuum deposition of the organic (bulk) molecules as contact on the molecularly modified substrate. To exploit these effects with general (inorganic) electronic devices, we developed a "soft" method to place a metal contact on top of the organic layer without damaging the organic molecules. With it we could produce a range of metal/MoL/semiconductor junctions, including Au/MoL/n-Si,[14] /n-ZnO,[43] and /n-GaAs.[44−46] All these junctions were electrically controlled by inserting a MoL at the interface, using disulfide adsorption to Au;[14] di-carboxylic acid adsorption on ZnO[43] and n-GaAs,[44] linear conjugated carboxylic acids to n-GaAs;[44] and functionalized C_{60} to n-GaAs.[46] We showed that this layer of small, polar organic molecules changes the junction's barrier height systematically, according to the free molecules' dipole moments.

Though most of the research in this area (also often included as part of "molecular electronics") is concerned with charge *transport* characteristics through molecules, we emphasize here the *electrostatic* effect of the molecular layer. Thus, we will argue (section 5.2) that electrostatic effects alone can explain a 6 orders of magnitude change in measured current. Such a conclusion is possible because we use relatively large area devices with extremely narrow (∼1 nm) films of organic molecules that show only average order. This makes (coherent) tunneling effects very unlikely, as is further discussed in section 5.1 together with the general applicability of the thermionic emission model.

Predicting the barrier height in a metal−semiconductor junction is still an open issue, after half a century of electronics research. The different models are reviewed in the theory part (section 2) and serve as basis for section 5.3. There we consider systematically all common explanations, and after concluding that none of them can explain our results, we remain with the major finding of this study, which is that the potential barrier is dictated by the interfacial interactions. This is based on an extensive study of the effects that adsorption of a set of dicarboxylic acid (dC) ligands on GaAs has on the barrier height of metal/MoL/GaAs junctions, when the substituent on the ligand is changed systematically. We further determine how the interfacial dipole is affected by the metal deposition mode, metal type, and doping type (section 5.4). The major conclusion that we reach is that the interfacial dipole is the result of combined interactions, between the metal, the organic molecules, and the semiconductor. The reader might find it more interesting to skip first the following theoretical section (section 2) and return to it only after/while reading section 5.3. Similarly, because section 5.1 is concerned mainly with considering (and rejecting) other approaches, it could be left for the second reading of the manuscript.

2. Theoretical Basis

We briefly review the major approaches accounting for the formation of a barrier for electronic transport in metal/semiconductor (Schottky) junctions,[31,47−49] as depicted schematically in Figure 1.

The two important energy levels to be considered are the Fermi level (E_F, which, in the case of a semiconductor, refers to the electrochemical potential of the electron) and the local vacuum level (E_{vac}, the energy of an electron at rest, just outside the solid, not bound to its lattice, but still within the range of the crystal's electrostatic potential). The difference between the two is the work function, ϕ.

The metal is characterized by its work function, ϕ_m. A semiconductor is characterized by its electron affinity, χ (i.e.,

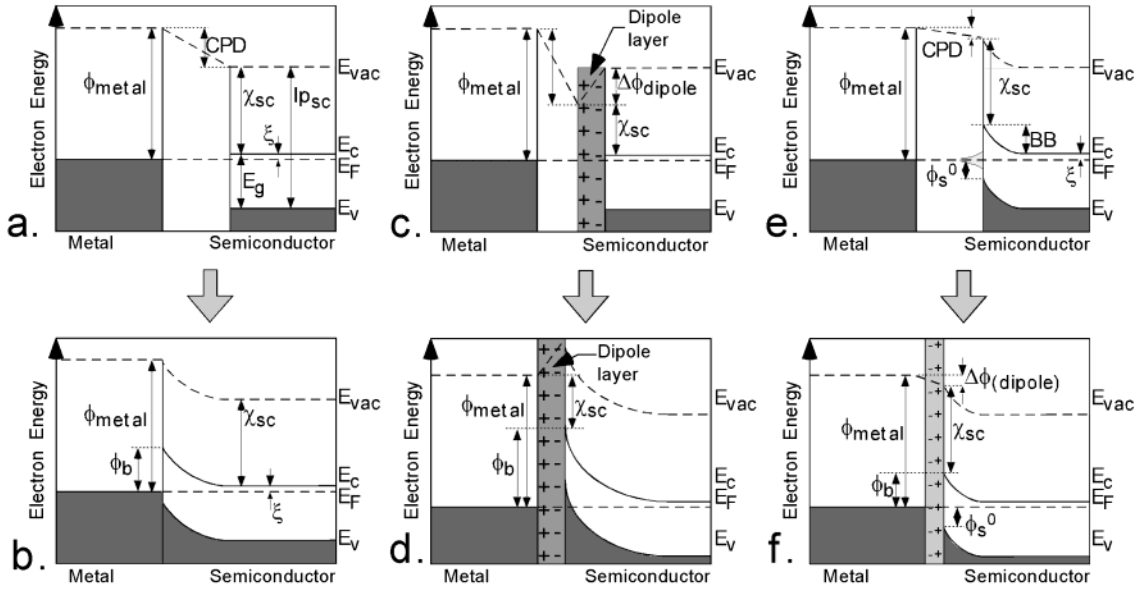

Figure 1. Schematic description of possible sources of the molecular effect on the junction's barrier height. The potential energy for one electron (*y*-axis) is plotted as a function of distance (*x*-axis) into the metal, left, or n-type semiconductor, right. The panels present situations before (a, c, e) and after contact (b, d, f), within the Schottky-Mott model with (c, d) and without (a, b) an added dipole layer at the interface, and for the Bardeen model (e, f). In panel (a), characteristic energy parameters of the semiconductor surface are presented as well (see text for more details).

the energy difference between the vacuum level, E_{vac}, and the bottom of the conduction band; cf. Figure 1a), and by its ionization potential, *Ip* (i.e., the energy difference between the top of the valence band and E_{vac}). All these quantities, work function, electron affinity, and ionization potential, are taken as positive values. The Fermi level in the bulk of the semiconductor is inside the forbidden energy gap, at $\xi^n = E_{CB} - E_F$ (for n-type) and $\xi^p = E_{VB} - E_F$ (for p-type). ξ is positive for n-type and negative for p-type and can be calculated from the semiconductor's net carrier density.[50]

If we connect the metal and semiconductor electrically, but not spatially (top panels of Figure 1), then their Fermi levels equilibrate because electrons transfer to the electrode with the larger (more negative with respect to the vacuum level) work function. As a result, an electrostatic potential is built up between the two electrodes, expressed as a difference in the local vacuum level at the two surfaces. This is the property measured as contact potential difference (CPD). We give CPD in eV, rather than in V, the units in which the quantity is experimentally measured, so as to simplify the following equations. For an n-type semiconductor CPD is then defined as

$$\mathrm{CPD}_L^n = \phi_m - \phi_{sc}^n = \phi_m - (\chi + \xi^n) \qquad (1a)$$

and for a p-type semiconductor as

$$\mathrm{CPD}_L^p = \phi_m - \phi_{sc}^p = \phi_m - (Ip + \xi^p) \qquad (1b)$$

where the subscript L means that this represents the situation in the light (see below).

If an external dipole layer is present (Figure 1c), then E_{vac} is taken outside this layer and a superscript "eff" is used with χ and *Ip* in eqs 1 to indicate that this is the effective parameter including any contribution due to dipoles, $\Delta\phi^{dip}$ (as drawn in Figure 1c and given in eq 8 below). Finally, the energy bands are commonly shifted at the semiconductor surface compared to their value in the bulk (Figure 1e), and this difference is the band bending (BB), which is taken positive for an n-type and negative for a p-type semiconductor with a depletion layer. Adding the contribution of BB to eq 1a, b we get the following relations:

$$\mathrm{CPD}_D^n = \phi_m - \phi_{sc}^n = \phi_m - (\chi^{eff} + \mathrm{BB} + \xi^n) \qquad (1c)$$

$$\mathrm{CPD}_D^p = \phi_m - \phi_{sc}^p = \phi_m - (Ip^{eff} + \mathrm{BB} + \xi^p) \qquad (1d)$$

where BB results from charges localized at the semiconductor surface. These charges can be neutralized under saturating suprabandgap illumination ($\mathrm{CPD_L}$) to result in near-flat bands (BB $\rightarrow$ 0). Eqs 1c, d then reduce to eqs 1a, b, which, therefore, are not limited to ideal semiconductors (Figure 1a,c) but are applicable to any semiconductor surface measured under such saturating illumination. Thus $\mathrm{CPD_L}$ allows extraction of χ^{eff} (Ip^{eff}) for n- (p-)type semiconductors, up to a constant, ξ^n (ξ^p), and the BB can then be calculated from $\mathrm{BB} = \mathrm{CPD_D} - \mathrm{CPD_L}$.

If we bring the metal and the semiconductor surfaces into direct physical (as well as electrical) contact (bottom panels of Figure 1), the two local vacuum levels need to match at this interface (in addition to the Fermi levels). The electrostatic potential is screened on the metal side due to the high density of free charges, but this is impossible on the semiconductor side (low number of charge carriers), leading to an electrostatic potential drop over a finite distance (~Debye length) into the semiconductor (over the space charge region). This is the basic Schottky−Mott model, and the electrostatic barrier for electron transport ($\phi_b^{i,S}$) is then defined by

$$\phi_b^{n,S} = \phi_m - \xi^{eff} \qquad (2a)$$

$$\phi_b^{p,S} = Ip^{eff} - \phi_m \qquad (2b)$$

The superscript i = n, p gives the doping type of the semiconductor, while the superscript S indicates that this is the barrier within the Schottky−Mott formalism. The subscript b stands for "barrier". Equations 2a,b indicate that a surface dipole layer (intrinsic or adsorbed, as in (c)) modifies the effective solid work function by a dipole-induced potential drop ($\Delta\phi_{dipole}$, see eq 8). Hence, it alters the net energy balance upon contacting (d) to modify the resulting barrier height.

Actually, relating the junction's barrier to the work function balance (Schottky−Mott model) represents only one extreme type of junction behavior, with the other extreme being the one where the (inter)surface states are the dominant factor controlling the barrier height, rather than the metal work function. This is the so-called Bardeen model[51] shown schematically in Figure 1e,f. The Bardeen case (regardless of adsorbed or intrinsic dipole layer) assumes that interface states, at a sufficiently high density, dictate the position of the Fermi level (Fermi-level pinning) at its neutrality level, ϕ_s^0 (relative to the top of the valence band). There are several possible origins for these states but all assume that contacting will not change the position of the Fermi level at the surface (now interface) and that, therefore, the CPD (in panel e) must fall over a thin interfacial layer (acting as a charged insulator; i.e., the result is the same as with a dipole layer, but the origin is different). This gives for the "Bardeen" barrier height ($\phi_b^{i,B}$, always a positive quantity):

$$\phi_b^{nB} = E_g - \phi_s^0 \tag{3a}$$

$$\phi_b^{p,B} = \phi_s^0 \tag{3b}$$

The two extreme cases of metal-dependent (eq 2) and metal-independent (eq 3) barrier heights are commonly related by an empirical factor, γ, weighing the two contributions:[51]

$$\phi_b = \gamma\, \phi_b^S + (1 - \gamma)\phi_b^B \tag{4}$$

Using eqs 2 and 3 we find for an n-type semiconductor:

$$\phi_b^n = \gamma(\phi_m - \chi^{eff}) + (1 - \gamma)\,(E_g - \phi_s^0) \tag{4a}$$

and for a p-type semiconductor

$$\phi_b^p = \gamma(Ip^{eff} - \phi_m) + (1 - \gamma)\,\phi_s^0 \tag{4b}$$

For a given semiconductor, γ is commonly extracted by plotting the barrier height against the metal *work function* (ϕ_m). Mead and co-workers[52] suggested that the relevant metal property should be its electronegativity, rather than the work function, and termed it the index of interface behavior, S. Here we used adsorbed molecular layers to modify χ^{eff} (Ip^{eff}) instead of varying the metal, so we used the measured CPD_L (eq 1a,b) to extract γ (see also eq 9). We extracted S by plotting the barrier height vs. the molecular energy levels (instead of metal ones), as demonstrated below in Figures 5−7 and presented in Table 2.

3. Experimental Section

3.1. Materials. *GaAs Wafers.* (100) n-GaAs wafers, Si doped to $(1-2) \times 10^{18}$ cm^{-3}, were purchased from AXT. (100) p-GaAs wafers, Zn doped to 1.7×10^{17} cm^{-3}, were purchased from ITME. Ohmic contacts were made on the backside of the wafers by evaporation of Au:Ge:Ni or Zn:Au for n- or p-GaAs, respectively, at the Brown center for submicron physics (WIS). The GaAs substrate was cleaned by a jet of methanol, followed by ozone oxidation for 10 min in a UVOCS apparatus. The oxide was removed by a 30 s dip in diluted NH_4OH (1:5), after which the sample was rinsed, without drying, in ACN, and immediately placed in the adsorption solution.

Ligands. The synthesis of the set of dicarboxylic (dC) ligands used here (cf. Figure 2a) was reported earlier.[53] The π electrons of the phenyl ring in the dC ligands are highly polarizable and change their distribution depending on the para substituent, to create a permanent dipole on the free molecule. The abbreviations used as molecule nomenclature are given in Table 1.

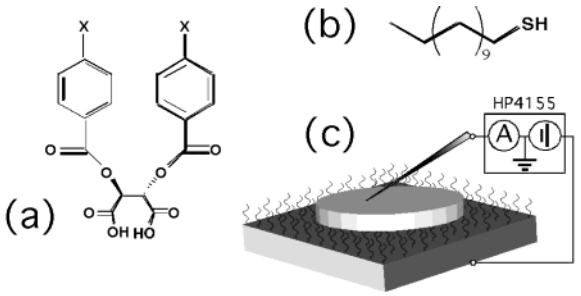

Figure 2. Chemical and structural formulae of the dicarboxylic acids (dC) used to construct the monolayers (a). Same, of the dodecanethiol (alkanethiol), used for the insulating layer (b). Schematic device structure (c).

TABLE 1: Physical and Chemical Information on the Substituted Dicarboxylic Molecules Used (cf. Figure 2a)

abbreviation	chemical formula[a]	polarity[b]	dipole moment (D[c,d])	LUMO energy (eV)	EN (eV)[e]
CN	Ph−CN	+ −	2.25	1.70	5.50
CF_3	Ph−CF_3	+ −	2.72	1.50	5.47
H	Ph	0	−3.45	1.52	5.15
Me	Ph−CH_3	− +	−4.00	0.60	4.54
OMe	Ph−OCH_3	− +	−4.42	0.20	4.49

[a] Ph represents the phenyl ring of the compounds, shown in Figure 2a. [b] This refers to the charge distribution of the substituted phenyl ring only, with the ring on the left and the substituent on the right. Note that there is additional strong charge withdrawal by the carboxyl groups. [c] The dipole moment refers to the whole molecule. The quantities were calculated by the PM3 method for the isolated, protonated dC molecules. [d] For dipole units see ref 67. [e] The (Mulliken) electronegativity (EN), is defined as (LUMO + HOMO)/2; see text.

Other Chemicals. 1-Dodecanethiol (>98%) was purchased from Aldrich and used without further purification. Acetonitrile (ACN) of extra dry grade (99.9%) was purchased from Biolab. Other solvents were analytical grade. Deionized water was used (18 MΩ). Au and Al were 99.999% pure and purchased from Holland-Moran and Johnson Matthey.

3.2. Sample Preparation. *Adsorption.* FT-IR (Bruker Equinox 55; transmission mode) shows that carboxylic acid groups bind to GaAs and more ionic semiconductors to produce the equivalent carboxylate (see also refs 54 and 55). The double binding group increases the adsorption constant.[55] A self-assembled layer of molecules (MoL)[22] on GaAs was made by overnight immersion in 1 mM ACN solution. For the methoxy (OMe) termination 0.5 mM + 4% (v/v) of water was required to accomplish adsorption.[56] After adsorption the samples were rinsed in clean ACN for 1 min. Alkanethiols are well-known to form a monolayer on noble metals, by releasing a proton, and forming an S−Au bond.[19,57,58] A MoL on Au was formed by overnight flotation of Au pads on a 2.5 mM ACN solution of 1-dodecanethiol.[59] ACN was used as a solvent instead of the commonly used ethanol[20,57] because Au films do not float on ethanol (vide infra).

Top Contact. Metal/MoL/GaAs junctions were made using several variants of the lift-off float-on (LOFO) procedure described in detail elsewhere.[59] It consists of peeling a ~60 nm thick, 0.5 mm diameter metal pad from glass or modified glass and letting it float on ACN + 0−50% v/v H_2O. The pads are then floated on the (molecularly modified) GaAs substrates. In the case of ligand adsorption on Au, the pads are first allowed

to float on the adsorption solution overnight and then transferred onto clean ACN to rinse off excess molecules, before floating them onto GaAs substrates. Immediate, flash heating of the (pad + GaAs) to 70 °C was found to stretch the metal film on the surface and is referred to as LOFO. Alternatively, slow heating (over a period of hours) in a vacuum oven (50−70 °C), is termed "slow" LOFO. Normally, the same ligands were adsorbed on 3−4 samples, with 3−5 pads on each sample, to produce 10−20 diodes for a given interface.

We will use the term "bare" (junction) to indicate a junction made as all the others, but directly on a freshly etched GaAs surface without any of the molecules of Figure 2 adsorbed onto it. The surface of the GaAs, without molecules, used to prepare the "bare" junction, is also exposed to the solvent, but only during the LOFO process (2−5 min), to minimize solvent adsorption on the surface. Other reference samples were prepared, using thermal evaporation of Au in a vacuum chamber, directly on the modified GaAs, instead of LOFO deposition. For this the adsorbed and rinsed GaAs samples were placed directly onto a 0.5 mm diameter shadow mask. A base pressure of 10^{-7} mbar was established within ~30 min. In the case of evaporation in an Ar atmosphere the Ar was let in through a needle valve up to a pressure of 10^{-5} mbar. Each type of molecule was adsorbed on only one sample, and evaporation was done on the 6 samples together, to produce 20−30 contacts on each sample. In the case of direct evaporation, the Au contacts were not annealed, in contrast to what was the case for the preparation of Au pads for LOFO, which were annealed immediately after evaporation. Au pads were stored up to a few weeks, until used for LOFO deposition. Al pads were kept in a desiccator and used within 1−3 days to minimize oxidation.

3.3. Characterization. *Quantum mechanical calculations*[60] were carried out as described elsewhere[45,61] using the GAUSSIAN 98 package[62] to find the configuration, charge distribution, and energy levels of the molecules (see Table 1). All calculations considered the carboxylic acid mode of the ligand (i.e., including a proton), rather than the (Ga) carboxylate, and were done for an *isolated* molecule ignoring condensed phase (MoL and substrate) effects. The semiempirical method PM3 (Parametric Method 3) was used for dipole moment calculations.[63] Dipole values presented here differ from those used in ref 44, where we used the literature dipole values of only the substituted phenyl parts of the molecules. For LUMO and HOMO calculation, the hybrid B3LYP[64] (Becke 3-parameter hybrid exchange with Lee−Yang−Parr correlation) density functional theory (DFT) method was used with the augmented Dunning cc-pVDZ[65] (correlation consistent polarized valence double-ζ) basis set. The calculations were checked against experimental values for a series of benzoic acid derivatives and found to be accurate. Therefore the calculated values used here are considered to be a better estimate for the dicarboxylic acids, for which no experimental values exist, than the values used earlier.

Surface potentials were measured using a Besocke Kelvin probe apparatus inside a N_2-filled glovebox. This technique[66] measures the contact potential difference (CPD, eq 1) between a vibrating reference Au probe and the sample. We used saturating, supra-band-gap illumination from a W−halogen light source to neutralize as much as possible the surface and space charges (cf. eqs 1a and 1b).

Current Voltage (*I*−*V*) *Curves.* Metal/MoL/GaAs diodes were contacted using a micromanipulator at room temperature, inside a dark, electrically screened chamber, in 30 mbar vacuum. *I*−*V* characteristics were measured between ±1 V in steps of 0.01 V, using an HP4155 semiconductor parameter analyzer with a 320 ms integration time. Bias was applied between ground and the back (ohmic) contact of the GaAs, and the current was measured between the micromanipulator, which contacted the leaf, and ground (see Figure 2c). For convenience, the *I*−*V* curves are drawn using the convention that forward bias is positive, i.e., in the first quadrant. Thus, the forward direction of the bias was defined depending on the conductivity type (i.e., the bottom contact was biased negative or positive for n- or p-type devices, respectively).

All LOFO-made contacts were checked by optical microscopy to verify their smoothness. Only smooth pads were used for electrical measurements. Such pads contain at most a few single large wrinkles, which we assume to have a minor influence on the current, due to their large resistance. *I*−*V* curves were measured until any effects from earlier light exposure of the diodes had decayed completely and the curves had stabilized. The barrier height was extracted (see section 4.3) from such stabilized *I*−*V* plots. The value that we give is the average of those obtained from 10−12 different pads on up to 3−4 different samples, with the reported error being the standard deviation of the data. In certain cases we excluded 1−2 strongly deviating data points from the averaging. We note that the RMS error within a given linear fit was negligible compared to the deviation between different *I*−*V* curves. The differences between *I*−*V* plots of the same junction type were rather large on a linear plot, but much smaller on a semilog plot, i.e., averaging must be done in log current terms and not directly in the linear terms were the high current (low barrier) data obscure the others.

4. Results

4.1. dC-Modified GaAs Surfaces. As reported briefly earlier,[14,44,45] we can insert a MoL into a solid junction to modify its barrier height, using the "lift-off float-on (LOFO) technique. Elsewhere we describe the details of the LOFO technique and the possibility of using it to form an intimate metal/molecule interface.[59] Here we focus on understanding the metal/GaAs junction that is formed by LOFO and on the way that the metal−MoL spacing as well as the semiconductor doping type (n and p) affect electron transmission across the semiconductor/metal junction.

The effect of the molecules on the Au/molecular film/GaAs junction was verified by systematically modifying the ligands that make up the MoL. The common ligand skeleton is shown in Figure 2a, and the five different substituents are listed in Table 1, with their abbreviations. Table 1 also gives the results of quantum chemical calculations of molecular quantities for molecules with the different substituent groups. The use of a series of molecules with identical binding group (to bind to the solid surface) and an identical bridging part between the binding group and the varying functional part, is crucial to distinguish between general molecular features (e.g., the insertion of a thin insulating film) and specific molecular parameters (e.g., changes in the molecule's frontier orbital energy levels or the molecular dipole). Therefore, each experiment was repeated for five different MoLs + a "bare" interface with no MoL adsorbed on the GaAs surface.

The adsorbed molecular layer (MoL) consists of roughly one monomolecular thick layer, as evident from both contact angle measurements (which show a distinct dependence on surface termination[59]) and IR spectra (the carboxylic acid stretch frequency shifts to a carboxylate one[55]). Ellipsometry data (see Supporting Information) and XPS measurements[54,68] indicate ~10 Å of natural GaAs oxides,[54,68] below a ~10 Å thick organic

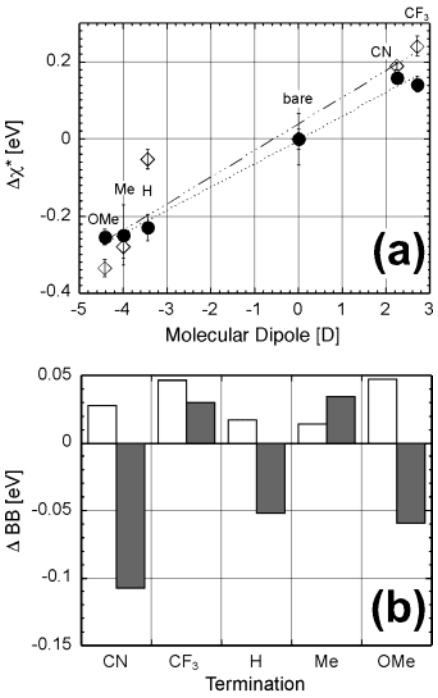

Figure 3. (a) Molecular film-induced change in surface potential, relative to that of the bare (MoL-free) surface, for molecularly modified n- (●) and p- (◇) GaAs (100), as measured by a Kelvin probe under illumination (yielding the electron affinity), plotted against the calculated dipole moments of the free molecules (Table 1). Values are averaged over 5−7 samples with the standard deviation as error bars. (b) Change in band bending (BB) of molecularly modified n-GaAs (empty bars) and p-GaAs (filled bars). The errors in the BB values (not shown, for clarity's sake) are in the order of a few tens of millielectronvolts. For the bare surfaces we measured electron affinities of 0.64 and 0.26 eV below the Au reference (i.e., CPD values of 4.36 and 4.74 eV, taking $\phi_{Au} = 5.00$ eV) and a lower limit of band bending of 0.23 and 0.16 eV, for n- and p-GaAs, respectively.

layer. Altough the thickness of the molecular layer (MoL) is somewhat larger than what is expected (7.7 Å) from calculating the thickness of a film of 10 Å thick molecules with a ∼50° tilt from the surface normal, the difference is not unreasonable in view of the difficulties in extracting data from ellipsometry measurements on this type of system.

The molecular effect on the electrical properties of the free surface was evaluated using the Kelvin probe technique and is presented in Figure 3. The top panel (Figure 3a) shows the effect of dC adsorption on the electron affinity of GaAs (100). The molecular layer can modify the electron affinity (χ) by up to 0.4 and 0.57 eV for n- and p-GaAs, respectively. For both doping types the effect correlates well with the dipole moment of the (isolated) molecule, and the two data sets follow more or less the same trend. The change in electron affinity is due to an *external* potential drop (see Figure 1c and discussion), yet adsorption can modify also an *internal* potential drop due to a change of charge density at the surface (Figure 1e). This is expressed as a change in band bending (BB) and given in the form of a histogram in Figure 3b. This shows that adsorption slightly increased the BB for n-type (by up to 50 meV) compared to the bare (oxidized) surface. Adsorption of the same molecules on p-GaAs resulted in a much stronger dependence on the specific substituent groups with a change in BB between +30 and −110 meV.

4.2. Current−Voltage (*I*−*V*) Behavior of Various Junction Types. Figure 4 shows plots of the logarithm of the (absolute) measured current vs the applied bias (ln *I* vs *V*) for the Au/dC/p-GaAs junction, a representation that allows viewing effects of small currents as well as changes in exponents. The six curves correspond to the junctions made with the five different molecular substituents plus that of the "bare" junction. Each curve is the *geometrical* average of about 10 measured curves. In the inset in Figure 4 we present the actual linear *I*−*V* plots of the junction. These show the expected nonlinear characteristics of these asymmetric junctions.

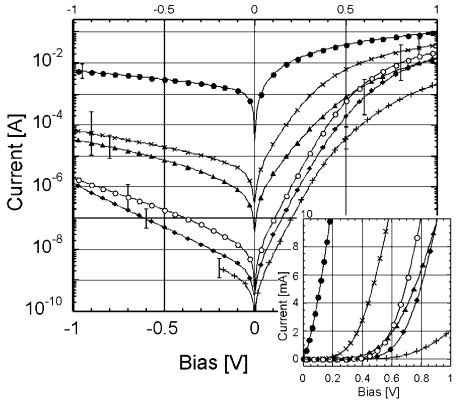

Figure 4. Current−voltage (*I*−*V*) curves for LOFO-made Au/dC/p-GaAs junctions. The *X*-axis gives the applied bias and the *Y*-axis is the current on logarithmic (main panel) and linear (inset) scales. These are two presentations of exactly the same raw data. For each molecular substituent ∼10 different diodes were made and measured, and the geometrically averaged *I*−*V* data are plotted as a single curve, for molecularly modified junctions with CN (●), CF_3 (×), H (▲), Me (○), and OMe (+) terminations and for the bare junction (◆). For clarity's sake the error bars (representing the actual span of the data) are presented, for each curve, at only one positive and one negative bias voltage. The bias polarity convention is that the bias is positive (forward) when the p-GaAs is positive. Because we calculated the geometrical average, the errors shown in the main panel are symmetric (and could be very large in the inset).

For a given bias in Figure 4, the current varied by up to 6 orders of magnitude depending solely on the small substituent group. The differences were fairly constant in the reverse bias range (parallel curves in the semilog plot) but decreased with increased forward bias. Similar analyses for n-GaAs revealed that the extent of the substituent effect was between 2 and 2.5 current decades. For a more quantitative characterization, we can extract the barrier height from the *I*−*V* curves, as described next.

4.3. Extraction of Barrier Height and Relating It to Molecular Parameters (S): n-GaAs. Because we get clear rectifying *I*−*V* characteristics, it is suggestive to analyze them in terms of a potential barrier for transport. The simplest way to view transport across metal−semiconductor junctions is as a thermally activated process (or thermionic emission) over the potential barrier in the space charge region on the semiconductor side of the junction:[31,50,69]

$$I = I_0 e^{-\phi_b/kT}(e^{qV/kTN} - 1) \quad (5)$$

where *I* is the measured current, *V* is the applied bias, ϕ_b is the barrier height (in eV), *q* is the electron charge, *k* is the Boltzmann constant, *T* is the temperature, and *N* is the so-called "ideality factor", which is discussed below. I_0 is the saturation current for a zero barrier. For $V \gg kTN/q$ the −1 term in eq 5 is negligible and the current−voltage curve has a simple exponential relation. Thus plotting ln *I* against *V* should be linear above ∼0.1 V (for room temperature) and is curved closer to 0 V.

TABLE 2: Extent of the Molecular Effects on the Barrier Height, and Its Correlation to Different Molecular or Surface Parameters

		correlation[c] (sign of linear slope[d])				
junction type[a]	BH span (meV)[b]	dipole moment	LUMO (S)	electronegativity (S)	CPD_L[e] (γ)	$CPD_L + BB$[f] (γ)
slow LOFO Au/n	107	0.89(−)	0.8 (−)	0.85(−)	0.988(+)	0.85(+)
LOFO Au + SC_{12}/n	135	0.6(−)	0.93(−)	0.85(−)	0.5(+)	0.6(+)
evap Ar Au/n	27	0.8(−)	0.97(−)	0.93(−)	0.8(+)	0.85(+)
evap vac Au/n	77	0.6(+)	0.998(+)	0.93(+)	0.6(−)	0.4(−)
LOFO Au/n	66	0.8(+)	0.985(+)	0.97(+)	0.8(−)	0.4(−)
LOFO Au/p	373	0.85(−)	0.93(−)	0.94(−)	0.92(+)	0.88(+)
LOFO Al/p	253	0.7(−)	0.85(−)	0.85(−)	0.8(+)	0.85(+)

[a] Top contact deposition mode; metal (Au, Al) and conductivity type of the GaAs (n, p). In all cases there was a MoL on the GaAs side (bare junctions were omitted) and only the second row includes an additional MoL of dodecanethiol on the Au side. [b] This is the absolute difference between highest and lowest barrier height for a given junction type, resulting solely by varying the substituent group on the inserted molecules (Figure 2a). Barrier heights are calculated from the experimental data (such as those shown in Figure 4). [c] The correlation of a linear regression of the measured barrier height as a function of the parameter stated in the column title (cf. Figures 5−7), using the free molecule (gas phase) data, given in Table 1 and the measured (free) surface work function of Figure 3a. The correlation equals 1 for perfect linear dependence. [d] The term in brackets is the *sign* of the slope of each regression, where the slope is identified as either S or γ (see text). Spaces between rows separate between junction types with inverted slope signs. Theoretically, the sign is expected to invert for opposite doping types. [e] The contact potential difference with Au under photosaturation (cf. Figure 3a). [f] Linear regression after accounting for the 'free' surface band bending (BB) contribution as suggested in eq 12.

The barrier height (ϕ_b) can be extracted from the intercept of a linear fit to curves such as those given in Figure 4:

$$\phi_b = -kT[\ln I_{int} - \ln(AA^*T^2)] \quad (6)$$

where $\ln I_{int}$ is the intercept of the (semilog) linear fit, and the argument of the second logarithm equals I_0 with A the contact area (=0.002 cm^2, for a 0.5 mm diameter pad); T is the temperature (298 K); and A^* is the Richardson constant which accounts for the transmission probability through the interface. Based on literature values for the effective electron and hole masses, $A^* = 8$ and 54 $A \cdot cm^{-2} \cdot K^{-2}$ for n- and p-GaAs, respectively.[50]

In Table 2 we summarize the barrier heights for the different junction types, extracted by fitting the measured ln I vs V plot between 0.1 and 0.4 V. The first column gives the extent of the molecular effect, as the difference between the highest and the lowest barriers extracted for a given junction, made using the different substituent groups. In the remainder of the table, we show the degree to which the change in barrier height with molecular substituent correlates with the gas phase molecular properties (i.e., dipole, LUMO and electronegativity as given in Table 1) and with the molecule-induced change in surface properties (the experimentally measured CPD; data also presented in Figure 3). The slopes of the plots from which the correlations are extracted are taken as the "index of interface behavior" (see discussion in sec 5.3). We use S and γ to distinguish between the slope of the plots of the barrier height vs *molecular energy level (S)* and vs molecule-induced changes in *surface potential (γ)*. For brevity, only the signs of the slopes are presented in Table 2, in brackets next to each correlation. The sign of the slope for a p-type material is opposite to the sign of the factor (S, γ), as can be understood from eqs 4a and 4b. We find that the barrier height data generally correlate best with the molecular LUMO, which is therefore used as the abscissa in Figures 5 and 6.The differences between the barrier height of the molecularly modified and the "bare" junctions for n-GaAs are given in Figure 5. It compares the barrier heights calculated from the measured $I-V$ curves of junctions with only a dC MoL at the interface (filled circles) to those of a junction with an additional C_{12} thiol MoL on the Au side (hollow diamonds). From this we see that a second MoL at the interface inverts the trend of the substituent effect. The same "opposite" trend was observed also for junctions lacking the extra C_{12} MoL on the Au but prepared by slow LOFO. This is presented by the dotted line, on the basis of the data given in ref 44. The slopes of the fitted lines are the S factors (with, in the case of p-GaAs, opposite sign).

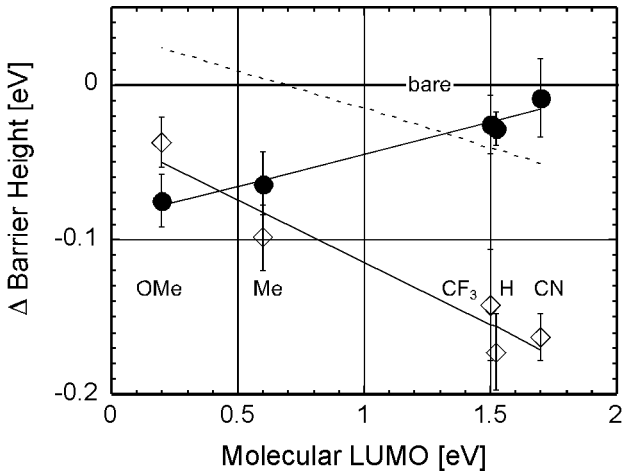

Figure 5. Dependence of the change in barrier height, with respect to the bare junction, of LOFO-made Au/dC/n-GaAs junctions on the LUMO level of the dC ligands, calculated for the isolated molecules (Table 1). The barrier height was extracted from the measured $I-V$ curves on the basis of the thermionic emission assumption (eq 6) and averaged over ~10 repeats with the standard deviation as the error bars. The plot compares the molecular effect for LOFO-prepared clean Au contact (●) to that of a (Au + spacer (dodecanethiol)) contact (◇). Data points are experimental values and lines are best linear fits, with their slope equaling S (see text and Table 2). The dotted line is the best linear fit for the Au/dC/n-GaAs junction made by the slow LOFO method.[44] For the bare junctions the following barrier heights were found: LOFO −0.78 eV; slow LOFO −0.71 eV; (LOFO + thiol) −0.91 eV.

The dramatic effect of the contact deposition mode demonstrated in Figure 5 suggests that we should compare also the results obtained with metal evaporation to those obtained with the LOFO procedure. In Figure 6 we show two sets of data obtained with evaporated contacts. We find them to be highly dependent on the exact evaporation conditions, as demonstrated by the effect of the atmosphere of the evaporator chamber on the barrier height of Au/dC/n-GaAs junctions. A 10^{-5} mbar argon (Ar) pressure (diamonds) virtually cancels the molecular

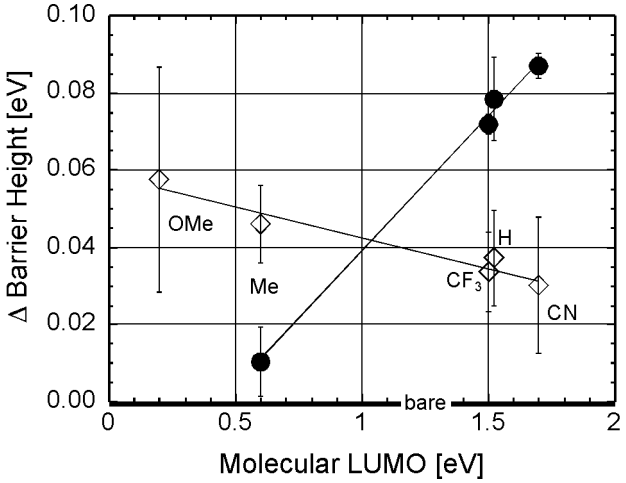

Figure 6. Dependence of the change in barrier height, with respect to the bare junction, of evaporated Au/dC/n-GaAs junctions on the calculated dC LUMO level (see Tables 1 and 2). The plot compares the molecular effect for evaporation at low base pressure (10^{-7} mbar, ●) to evaporation under Ar atmosphere (10^{-5} mbar, ◇). Data points are experimental values (for details, see legend to Figure 5), and the lines are best linear fits. For the bare junctions the same barrier height of 0.60 eV was found for both types of junctions.

expression in the barrier height, possibly even changing the direction of the effect again, compared to a one-time result of evaporation at 10^{-7} mbar base pressure (circles). The linear fits of Figure 6 are done as in Figure 5, showing a good correlation with the LUMO level (*S* factor).[70]

4.4. Relating the Barrier Height Data to Surface Parameters (γ): p-GaAs. Figure 7 shows data for p-GaAs and compares the electrical effect that the adsorbed dC has on the surface and on the interface. The junction barrier height (*Y*-axis) for LOFO-made Au (circles) and aluminum (Al, diamonds) junctions is plotted against the difference in work function between Au and dC-modified p-GaAs[71] (*X*-axis, same data as in Figure 3a). Symbols represent measured data and the line is a linear regression to the data. The points of the CF_3-substituted MoL and the "bare" samples were excluded from the linear regression, as they are clearly an exception (see 5.3.c in the Discussion). For comparison, the Au/dC/n-GaAs results are given only as a trend line (dashed line, same BH data as the circles of Figure 5 but different abscissa).

Figure 7 is a presentation of our data that is analogous to the one commonly used to present barrier height data, obtained under UHV conditions for junctions of the same semiconductor with different metals,[72] vs the work function of the contacting metal (Figure 7, inset, symbol X). *For illustrative purposes only*, as we have only two entries (for Al and Au), we give in the inset an example of such a plot, with the metal work function as abscissa. As noted above, the slope of such plots, the index of interface behavior, γ, expresses the extent to which the junction barrier height depends on the metal work function ($\gamma = 0$ for a barrier height independent of metal work function). The only difference between Figure 7 (main panel) and the traditional plot (inset) is that in the main panel we vary the molecularly modified work function of the *semiconductor* (approximated by CPD_L; cf. eq 1a,b), rather than the *metal* one. The relation between these two presentations is further discussed in section 5.3.a. For molecularly modified p-GaAs we get $\gamma = -0.68$ and -0.48 for Au and Al, respectively, which should be compared to the literature value of $\gamma = 0.1$ for vacuum deposition of metals on GaAs.[51] From the inset we see that there is almost no effect of the metal type on the barrier height for

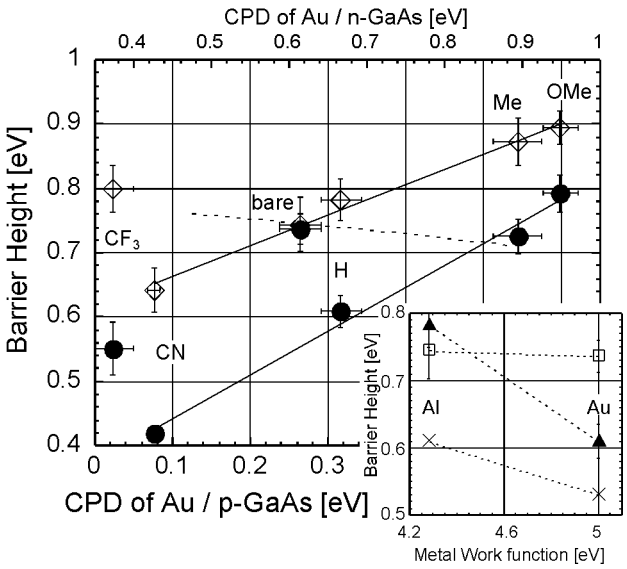

Figure 7. Dependence of the barrier height (extracted as described in the legend of Figure 5) of LOFO-made Au (●)/and −Al (◇)/dC/p-GaAs junctions (*Y*-axis) on the contact potential difference under illumination of the free molecularly modified p-GaAs surface, with respect to Au (CPD_L; bottom *X*-axis). Lines are best linear fits (excluding the data points for the CF_3-modified and bare junctions; see text). Their slope equals $-\gamma$ (cf. Table 2 and eq 9). For comparison the results for LOFO-prepared Au/dC/n-GaAs, from Figure 5, are shown as well (line-fit only, slope = γ), referred to the top *X*-axis. Inset: The barrier height of bare (□) and molecularly modified (H termination, ▲) junctions plotted against the work function of the metal (same BH data as given in main panel data). For comparison we plot also the BH of p-GaAs with the two metals produced under UHV conditions[72] (X).

the "bare" junction (hollow squares), whereas for the dC-modified junction (e.g., with H-termination; triangles in the inset), the Al−Au difference is almost 0.2 V. This is a real effect, as can be seen from the difference between the two fitting lines in the main figure.

4.5. Other Characteristics of the *I*−*V* Curves. According to eq 5, plotting the logarithm of the absolute current against the applied bias should give a straight line with a slope of $q/(kTN)$ for the forward bias and a zero slope for the reverse bias, for $|V| \gg kT/q$. The curves such as those presented in Figure 4 are generally not linear in the forward bias range and have slopes smaller than q/kT (i.e., $N > 1$). Also in the reverse bias range the curves deviate from a horizontal line, expected theoretically for pure thermionic emission. However, this is quite common for practical Schottky diodes.[31,69] There are a large number of explanations for such behavior, but unfortunately, often there is no clear experimental test to distinguish between them.

Nevertheless, to gauge the degree to which use of the thermionic emission model is justified for molecularly modified junctions, we give in Table 3 the values of the ideality factor and of the series resistance. The values are average values for a given junction type, regardless of molecular termination. The ideality factor was extracted from the slope of the best fit to the ln *I* vs *V* plot in the range + 0.1 to 0.4 V. The series resistance was extracted from a linear fit to a differential conductance plot ($G = dI/dV$). Werner[73] showed that a plot of G/I vs *I* should be linear with a slope equal to the series resistance. We note that we linearly fitted the high current range (where we assume the series resistance is most pronounced) and that in a large part of the curves a clear change in curvature is observed for lower currents (at lower bias).[74] This curvature

TABLE 3: Ideality Factors (N) and Series Resistances (R_s) for the Different Types of Junctions

junction type	N^a	err N^b	min R_s^c [Ω]	max R_s^c [Ω]
Au slow LOFO n	2.97	1.44	10^3	3.9×10^3
Au + SC_{12} LOFO n	3.00	0.43	200	1.1×10^3
evap Ar n	1.78	0.22	3	8
evap vac n	1.79	0.36	3	13
Au LOFO n	1.97	0.48	6	23
Au LOFO p	2.07	0.50	7	53
Al LOFO p	2.45	0.35	0.45×10^3	14.4×10^3

[a] N was calculated from the slope of ln I vs V plot as in eq 5 and averaged over al all the diodes made, regardless of the molecular termination. [b] Standard deviation. [c] R_s was calculated using the differential conductance method[73] (see text, section 4.5). The min and max values refer to an average over a given junction type, excluding exceptional values. Spaces between rows separate distinctive junction behaviors.

means that the high ideality factor measured at moderate forward bias (0.1−0.4 V) cannot arise from series resistance alone and that an additional bias-dependent mechanism is present. We will address this point in detail in a forthcoming publication.[74]

The ideality factors range from 1.8 to 3, which suggests either an additional mechanism for electronic transport across the junction (apart from pure thermionic emission for which $N = 1$) or a spatially inhomogeneous barrier height.[86,87] Still, this analysis brings out the large variation between the different junction types. Evaporation and LOFO with n-GaAs gave the smallest ideality factor (nearest to ideal), whereas the slow LOFO and LOFO + additional MoL on the Au side were the least "ideal". The junctions to p-type were intermediate. Comparing Tables 2 and 3 we see that for n-type junctions, the less ideal is the junction (larger N), the larger is the ability of the molecules to modify the barrier of the junction ("BH span" in Table 2).

The series resistance values showed much larger variation, ranging from a few ohms to megaohms. This is especially apparent for the case of double adsorption (and, to a lesser extent, for Al/p-GaAs), where distinct series resistance values were typical for different dC terminations. For the other junction types, the series resistance correlates with the trend in ideality factor; i.e., the lower the ideality factor, the lower is the series resistance. This trend cannot be attributed to the well-known increase in the "ideality" factor due to series resistance, as the series resistance has almost no effect on the ideality factor below 0.5 V (which is the region over which the fit was made). We will correlate these experimental facts with molecular processes in the next section.

5. Discussion

We first consider in how far the "classical" thermionic emission model can be applied to the metal/MoL/GaAs systems, studied here, and compare them to UHV-prepared metal/GaAs junctions (5.1). We then consider the importance of an interfacial dipole layer for such junctions (5.2). In the following parts we look for possible correlations between our experimental results for junction barrier heights and parameters of the free molecules or free surfaces (5.3). We conclude that the single most likely cause for the observed effects of the molecules is interfacial charge redistribution (5.3.c to 5.3.d) and then show how this explains the differences observed between n- and p-GaAs and between the different modes of metal deposition (5.4). The first discussion sections (5.1 to 5.3.b) lay the basis for the following section (5.3.d to 5.4) where we report on the more novel conclusions. Thus, the busy reader might go directly to section 5.3.d and return later to the background section (2) and the opening of the discussion.

5.1. Applicability of the Thermionic Emission Model. We now consider in how far the barrier height, obtained by analyzing the data as reflecting a thermally activated process (generalized thermionic emission), can measure molecular effects.

5.1.a. Comparison to Literature Values for UHV-Made Au/GaAs and Al/GaAs Junctions. The barrier height that we extracted from the measured $I-V$ curves of the "bare" junctions can be compared to values reported for UHV-prepared junctions. For n-GaAs the barrier heights were 0.78, 0.60, and 0.91 eV for LOFO-, evaporation-, and (LOFO + thiols)-prepared junctions, respectively. For UHV-evaporated Au on n-GaAs (100)[75] the measured barrier height is 0.92 eV.

For p-GaAs (100) the barrier height of LOFO-prepared junctions was 0.74 eV for both Au and Al, a value that can be compared to 0.53 and 0.61 eV for UHV evaporation-prepared junctions with Au and Al, respectively.[72] The ideality factors for all these (solution-made) junctions are generally much higher than those obtained for UHV-made diodes, where the ideality factor is normally below 1.1. In view of these high ideality factors, the barrier heights that we calculate from our data should be viewed as *effective* ones within the pure thermionic emission model.

Most of the barrier heights that we get are smaller than those reported for UHV-prepared junctions, closer to half the band gap value (the exception for "LOFO+thiols" is attributed to the tunnel barrier that is added because of the layer of "spacer" alkyl molecules; see 5.1.d). Such behavior is commonly explained by the presence of a high concentration of defects at the interfaces of such junctions, which pins the Fermi level close to midgap.[76] The lower barrier heights fit with the fairly high ideality factors that we get. Therefore it is the more striking that, notwithstanding such nonideal interface conditions, we find clear molecular effects on the *effective* barrier height.

This tells us that the idealized thermionic emission model as such cannot, by itself, explain electronic transport across these junctions. Indeed, the nonlinear log I vs V plots (Figure 4) indicate that there are additional mechanisms, especially at higher forward biases, which will be analyzed elsewhere.[74] Here it suffices to note that, regardless of the actual transport mechanism, the barrier that we extract is characteristic for a general thermally activated process and represents the thermal barrier for electronic transport, modified by the $\exp(qV/NkT)$ term. As such, these *effective* barriers are not necessarily *the* "thermionic emission" barriers. Even if the net values might be shifted by a factor (for example, due to an incorrect prefactor AA^*, as considered in section 5.1.c), they reveal the molecular *trend*, which is the goal of this study.

5.1.b. Interface Behavior of dC Molecules Compared to Inorganic Treatments. Irrespective of the origin of the molecular effect, we note that the changes in barrier height that we obtain (up to 0.4 eV) are rather large, considering the wet conditions used to prepare the junctions. Even the junctions prepared by Myburg et al.[75] by UHV evaporation of the metal on MBE-grown GaAs, were fairly pinned. For example, to overcome Fermi level pinning on GaAs(100) Brillson et al. used As capping to protect the GaAs(100) surface from ambient oxidation or reconstruction. Only by taking such precautions could they find a significant difference in barrier height between Au/ and Al/n-GaAs (100).[76,77] In further work they showed that deliberate misorientation (2° off the (100) plane) is sufficient to move the Fermi level toward midgap by 0.5 eV for Al on

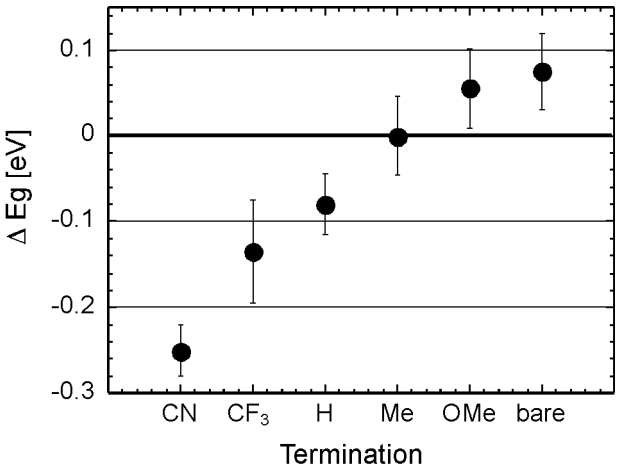

Figure 8. Sum of the experimentally extracted barrier heights for LOFO-prepared Au/dC/n- and p-GaAs junctions, for different molecular terminations. Theoretically, this sum should equal the band gap of the semiconductor (see eq 7). The *Y*-axis gives the deviation of this sum from the room-temperature band gap of GaAs ($E_g = 1.424$ eV). Barrier height data are taken from Figure 5 (n-GaAs) and Figure 7 (p-GaAs). The error bars are the sum of those of the barrier heights for the junctions with p- and n-GaAs.

n-GaAs, with a much smaller effect for Au.[78] In view of this we can expect that the extent of barrier height modification by molecular adsorption can be increased even further by, for example, junction preparation in an inert atmosphere and in clean room conditions.

5.1.c. Justification of the Use of Nominal Contact Area and Richardson Constant. In view of the conclusion from section 5.1.a, we need to scrutinize the validity of using the nominal contact area (A)[79] and the literature value for the Richardson constant (A^*), to extract the barrier height from eq 6. Measuring both types of doping allows testing the relation[51]

$$\phi_b^n + \phi_b^p = Ip^{eff} - \chi^{eff} \equiv E_g \qquad (7)$$

Equation 7 results directly from summing eqs 2a and 2b, for the Schottky−Mott case, with identical results for the Bardeen case (eqs 3a and 3b), *assuming that the relation between surface and interface properties is not affected by doping type*.

Hence, we present in Figure 8 the difference between the measured energy gap (i.e., the sum of the barrier heights) and the actual room temperature energy gap for GaAs (1.424 eV). From it we see that for the bare junction the above-stated assumptions are fairly well justified ($\Delta E_g \sim 0.07$ eV). In addition, the results for junctions with a MoL of molecules with Me and OMe termination were fairly close to those of the bare ones, whereas junctions made with a MoL of molecules with the other substituents yielded a sum of barrier heights considerably smaller than the forbidden gap. Considering eq 6, we see that if the actual contact area is smaller than the nominal one (as is likely to be the case for slow LOFO-prepared junctions; see discussion of Figure 9, below), this should lead, for both doping types, to larger effective (apparent) barrier heights. In such a case the difference plotted in Figure 8 should be positive. An interface-insulating layer with an additional tunneling barrier will have the same effect.[14] On the other hand a sum of barrier heights smaller than the band gap can be due to image force lowering of the barrier (the net difference could be larger than 0.1 V)[51] or to the highly doped n-GaAs that we used,[69] where, at room-temperature charge transfer by tunneling through the space charge can be significant. In such case one can still use eq 5 to describe the current, but I_0, the zero barrier current term, is now smaller.[31]

The finding that most of the data in Figure 8 show a negative deviation confirms our assumption of substituent-independent contact area and Richardson constant. The use of nominal values for these parameters can add a (constant) error of tens of meV to the absolute calculated BH values. Next we will consider the possible contribution of tunneling to the calculated barrier.

5.1.d. Possible General (Passive) Molecular Effects on the Metal/MoL/GaAs Barrier Height. If the MoL serves as a barrier for electronic transport (as was the case in some early work with LB films[80]) the resulting junctions should give a higher BH value than those without molecules (bare). This type of behavior (in addition to molecule-dependent one) was found for the higher quality MoLs on Au, used for Au/MoL/Si junctions.[14] This effect should be rather independent of molecular substituent and expressed as a *positive* difference in Figure 8. Yet the results of Figure 8 are both positive and negative and the value for the bare junctions is the *highest* (whereas we would expect it to be the lowest due to the expected smaller tunneling barrier compared to a junction with MoL). In addition, we can look at the position of the BH for the bare junction (BH_{bare}) compared to the MoL-modified ones (BH_{MoL}) (Figures 5−7). We see that BH_{bare} was between the BH_{MoL} values for p-GaAs (Figure 7), whereas for n-GaAs BH_{bare} is either larger than BH_{MoL} (for LOFO-made junctions, Figure 5) or smaller than BH_{MoL} (for evaporated junctions, Figure 6). The last case is what we would expect by if the barrier were one of simple tunneling through a dielectric. Thus, although it is possible that tunneling plays a role in the transport across the barrier in all the junction types, it does not dominate the process and cannot explain the molecular dependence in Figures 5−8.

Still, the results shown in Figure 8 also suggest a trend that is not yet explained. In the following, we address this issue. One possibility is that the molecules affect the barrier simply by the extent of coverage (or by the effective area they leave for direct semiconductor/metal contact; see also Figure 9 and discussion below) but do not play any electrically active role. For this to be true we expect a given molecular termination to increase the barrier (if it makes a well-packed MoL) for *both* doping types. This is contrary to what we find (cf. dotted line in Figure 7). In addition, surface characterizations indicate that the coverage is similar for different substituents (see section 4.1). A simple explanation for the trend in Figure 8 is the larger extent of the molecular effect on p-GaAs than on n-GaAs (e.g., the CN termination decreases the barrier height for p-type more than it increases that for n-type; see the "BH span" entry in Table 2 and discussion in section 5.4.d), violating the basic assumptions of eq 7 of dopant-independent surface characteristics.[51] In summary, Figure 8 points to an active, electrical role of the molecular layer at the interface, the basis of which is explained next.

5.2. Dipole Layer at an Electrical Junction. *5.2.a. Electrostatic Effect of an Interfacial Dipole Layer on the Barrier Height.* The effect of the interfacial molecular layer on the barrier height can be understood by considering the electrostatic balance across the interface (for an extensive review see ref 31). Intuitively, one could think that the molecular layer is the dominant barrier for electronic carriers. Though this is true for two metal contacts, it is not the case when one of the electrodes is a semiconducting one, with an "intrinsic" barrier due to the space charge region on the semiconductor side of the interface (cf. section 2 and Figure 1a,b). In the middle of Figure 1 we show the effect of an additional dipole layer at the interface.

Such a dipole layer is analogous to an (additional) parallel plate capacitor, and the potential energy drop over it ($\Delta\phi_{dip}$) can be estimated by[48,66,81]

$$\Delta\phi_{dip} = \frac{q\mu \cos\theta}{A\epsilon\epsilon_0} \quad (8)$$

where μ is the molecular dipole moment (C·m), which has an average tilt θ from the normal, A is the area per molecule (m^2), ϵ_0 is the permittivity of vacuum, and ϵ is the dipole layer's dielectric constant (derivable from the molecular polarizabilities, in the case of a molecular MoL, using the Clausius−Mosotti relation).[48,66,81] Note that $\Delta\phi_{dip}$ is taken positive if its positive pole points to the semiconductor; i.e., in Figure 1c,d it is negative.

The potential drop over the surface dipole layer can be viewed as changing the native electron affinity (for a given semiconductor surface) or work function (for a given metal surface) into an effective one (cf. Figure 1a,c, χ, and χ^{eff}, respectively). From eq 1 we see that such an added dipole layer should affect the CPD measurement as is indeed demonstrated in Figure 3a. We can compare the measured change in the induced potential, $\Delta\phi_{dip}$, to a calculation based on eq 8, with dipole values from quantum chemical simulations ($\Delta\mu = 7.15$ D[67]), a molecular footprint of 40 Å^2, $\theta \approx 55°$, and $\epsilon = 4$.[82] This way we find that the measured effect is about half of the theoretically calculated one. This is a reasonable result, in view of the nonideal character of the MoL and rough estimate of ϵ, which may be improved by taking into account additional effects such as depolarization.[66,81]

Actually, any measured work function (even on the cleanest UHV surfaces) includes a contribution of intrinsic surface dipoles, mostly due to surface reconstruction or the "spill-out" of the electron wave function in a metal. The latter leads to negative charge outside the metal, giving an outward pointing dipole, which "contains" the "free" electrons within the metal.[32,48] The pure physical effect of such a dipole at the interface can be derived in a rather straightforward manner from basic electrostatics and semiconductor physics[31,66] and was found experimentally by inserting a foreign atomic layer into the interface.[83−85] The novel aspect of MoL-modified junctions is its chemical nature, and in particular the possibility of a molecular entity making up the dipole.

The dipole effect for the noncontacting surface is sketched in Figure 1c, showing that a dipole that points into the semiconductor (positive charge on the unbound side of the MoL) decreases the semiconductor's effective electron affinity. In the case drawn it increases the contact potential difference (CPD) between the surface and the metal. If these two surfaces are brought into direct physical contact (Figure 1d), the larger CPD is now expressed as a higher barrier. This barrier will probably be significantly smaller than that due to a (molecular) continuous, insulating film. However, as the molecular layer is very thin, it is rather transparent to electrons because of tunneling, unlike the thick (>20 nm) space charge region in the semiconductor. In this respect we can view the semiconductor electrode as a transducer, translating small differences in charge distribution within a molecule into changes in charge distribution over a much larger distance, which are then expressed in variations of net current across the junction.

5.2.b. Influence of Defects on How a MoL Affects the Barrier Height. If the effect of the MoL is an electrostatic one, then this allows us to ignore questions of defects (pinholes) in the organic MoL, because the dominant barrier is now the semiconductor itself. This is rather different from the more common approach toward "molecular electronics", where the molecular functionality relies on the transmission function of the molecule, something that can easily be obscured by parallel short-circuit defects. In contrast, electrostatic effects concern potentials, which will not change abruptly.

If we view pinholes in the MoL as surface defects, we can use a model presented by Tung.[86] He showed that, as long as the dimensions of the pinholes are smaller than the semiconductor depletion width (20 and 60 nm for n- and p-GaAs, respectively), they are screened by the neighboring potential.[86] Another way to view the issue is to recognize the difference in the spatial extension of the electrostatic effects of an isolated dipole and a layer of dipoles. In the latter case the effect will extend from the domain, roughly out to the lateral domain dimension. Thus, if the pinhole diameter is less than the lateral size of the 2-D dipole domains, formed by the molecules, these dipole domains will affect the electrostatic potential in and around the pinholes (cf. refs 31 and 32). Even for larger area defects their contribution will be largely attenuated by the surrounding, averaged potential, although the larger the defect area, the more dominant it is.

Still, it is clear that this situation with a pinhole-rich MoL will lead to a nonuniform barrier height, something that is known to lead to a bias dependence of the $I-V$ characteristics (high ideality factor, cf. refs 86 and 87). This could account for part of the high ideality factors we get. An analysis of this, which is beyond the scope of this paper, will be presented elsewhere.[74]

5.2.c. Origin of Interfacial Dipoles; Failure of Noninteracting Solid Models. The exact mechanism dictating the barrier height at a metal−semiconductor junction is under discussion even today.[31] Thus, for example, in two distinct disciplines, that of inorganic silicides[31] and metal/organic junctions for OLEDs,[32] it has been noted that the two idealized, extreme models described in section 2, the Schottky−Mott and the Bardeen ones, fail to predict the actual junction barrier heights. The basic flaw is thought to be that the models are based on *noninteracting* solids. Indeed, experimental evidence is accumulating for strong charge transfer at metal/organic interfaces.[32] The data for metal deposition on molecules or vice versa, are interpreted in terms of interface dipole formation, which can affect the barrier for injection considerably (cf. Figure 1), thus affecting OLED efficiency. The molecules can interact with the metal in several ways, viz. metal polarization, coupling of electronic states, partial charge exchange (ionic bond formation) or formation of new chemical species.[32] This suggests that microscopic charge distribution (resulting in interfacial dipoles), over and beyond bulk electrostatic balance alone, can dictate the barrier height at the interface.

5.3. Correlating Barrier Height with Molecular Parameters. Which are the molecular parameters that influence the barrier height? Such parameter(s) should fulfill two criteria: (i) the change in the parameter should correlate reasonably well with the change in measured barrier height of junctions made with MoLs with different molecules, and (ii) the correlation should reflect an effect that can be explained physically. In the following we will analyze our barrier height data using three approaches, viz., work function, surface states, and bond polarization, and check the above-mentioned correlation. We find that for some of the junctions the correlation is best with work function-related (and free surface states related) parameters, whereas for others a bond-polarization model fits better. In section 5.4 we will explain the origin of this difference.

5.3.a. Barrier Height as a Function of GaAs (Surface) Work Function (Schottky−Mott View). We can relate the molecular effects on the surface properties and those on the interface by

plotting the measured barrier height against the molecularly modified CPD_L (as we did in Figure 7), rather than against the commonly used metal work function (Figure 7 inset). We will now show that the slope of such a plot gives the γ factor of eq 4. Comparing the expressions for CPD_L (eqs 1a and 1b) and for the Schottky−Mott barrier height (eqs 2a and 2b) shows them to be identical except for ξ, and a minus sign for p-type (eqs 1b and 2b). Therefore we can combine eqs 1, 2, and 4 to get

$$\phi_b = \pm \gamma(CPD_L + \xi) + (1 - \gamma)\phi_b^B \quad (9)$$

where the minus sign refers to the p-type case. Equation 9 shows that the slope of a plot of the barrier height against the measured CPD_L between metal and semiconductor should be positive ($=\gamma$) for n-type and negative ($=-\gamma$) for p-type. The γ signs in Table 2 show that all the four bottom junctions give a sign opposite to that expected (as will be discussed further in section 5.4.a). In terms of absolute values, most of the n-GaAs junctions gave a γ factor in the range of 0.1, similar to the 0.07 value for UHV-made n-GaAs[51] and 0.08 and 0.10 for n- and p-GaAs (100), respectively.[75,88] In contrast, the molecularly modified Au/p-GaAs junctions gave a remarkably high γ factor (up to 0.51; cf. Figure 7). This value is even higher, 0.68, if the CF_3 entry is excluded, justification for which appears in section 5.3.c.

Molecular adsorption also increases the dependence of the barrier height on the metal, as compared to the effect of metals on bare junctions (see inset to Figure 7). Although we have used only two metals, we note that with molecules the difference between them is in the direction expected for the metal work function (cf. eqs 4, which yield $\gamma > 0.15$), whereas there was practically no metal effect for bare junctions. These results are of interest in view of Fermi level pinning. Although Fermi level pinning has often been treated as an *intrinsic* property of the semiconductor, Brillson[71,77,78] and Tung,[31] among others, have argued that pinning at the metal/semiconductor interface results from the *interaction* between the phases that form the junction and the subsequent bond formation between the metal and the semiconductor. The inset to Figure 7 shows that, starting from a highly pinned interface, insertion of a poorly organized layer (~1 nm thick) of small molecules apparently buffers the metal−semiconductor interactions. This unpins the surface to an extent, which is even larger than that achieved in UHV ($\gamma = 0.1$).[75,88] Actually, already in 1965 Cowley and Sze suggested that evaporation on etched rather than cleaved surfaces produces a larger γ factor due to a thicker interfacial layer.[51]

5.3.b. Importance of "Free" Surface States (Bardeen View) for Barrier Heights.

5.3.b.1. Molecular Effect on "Free" Surface States. In contrast to the surface work function approach, it is very common to attribute the height of the *interfacial* barrier to electronic states existing on the "free" *surface* of the semiconductor (Figure 1e,f). Before considering the relation to the barrier height, we should first consider the molecular effect on the "free" surface, as presented in Figure 3. We see that adsorption can significantly reduce the band bending for p-GaAs whereas that of n-GaAs was fairly insensitive to the presence of molecules on its surface. However, this effect on the band bending is very sensitive to the initial conditions, i.e., to the exact chemical surface treatments before adsorption. For example, in ref 26 the opposite trend was found, i.e., adsorption of the same dC molecules considerably reduced "free" surface band bending for n-type, and less so for p-type. There we showed that the lack of effect on the surface of an additional set of low-doped n-GaAs samples is not necessarily due to the electrical interaction (i.e., filled vs empty surface states) but could be simply due to a density of surface states that is so high that molecular adsorption is not sufficient to change the net surface density significantly.

The major difference between the work presented in Figure 3b and that in ref 26 is that a different etching procedure was used, ammonia, rather than Br_2/KOH etch,[89] resulting in a different "bare" surface. Although this is unlikely to change the intrinsic surface levels of the GaAs (100), it is very reasonably that the different (inorganic) chemical treatments leave different terminations on the surface (e.g., hydroxyls or protons, cf. ref 42). Therefore, when the molecules are deposited from solution onto the surface, they will interact differently with differently etched surfaces.

The differences in the surface electronic properties show up also in the much smaller net band bending of the bare surface after ammonia etch (~0.2 eV) than after Br_2/KOH (~0.6 eV)[26,54]). Probably the ammonia treatment used here "cleans" the surface states, which were, after the earlier treatment, available for interaction with the molecules. As a result a surface is left with a residual amount of states that is rather insensitive to the binding.

The change in BB of p-GaAs (Figure 3b) is enhanced for molecules at the extremes of the LUMO scale (Table 1). This dependence can be understood in view of the two reported surface states levels of GaAs, at 0.2 and 0.8 eV above the valence band.[26,77] The LUMO effect suggests that the high LUMO substituent (e.g., CN) interacts with states near the valence band whereas low LUMO substituents (e.g., OMe) interact with empty states closer to the conduction band. Ligands with intermediate energy levels have no states to interact with and, thus, have a small effect on the band bending.[26]

5.3.b.2. Effect of "Free" Surface States on Junction Barrier Heights. When using eq 4 to extract the index of interface behavior, one normally regards the Bardeen barrier height (ϕ_b^B, right term of eq 4) as the outcome of the fitting, with no direct experimental verification. Kelvin probe data can be used also to elucidate the contribution from surface states to the barrier height.

For this we relate the free *surface* band bending and the *interface* barrier height by identifying ϕ_s^0 with the measured band bending of the free surface, BB; cf. Figures 1e,f and 3b). For the free surface the position of the Fermi level is approximately at the center of the energy distribution of the surface states (ϕ_s^0). This assumption is correct if the density of surface states is sufficiently high, and then

$$\phi_s^0 = (E_g) - BB - \xi \quad (10)$$

where the energy gap, E_g, needs to be included only for n-type semiconductor. Inserting eq 10 into eqs 3a and 3b, we get a relation between the barrier height in the limit of the Bardeen model (ϕ_b^B) and the measured band bending (BB) for the molecularly modified surface:

$$\phi_b^B = \pm(BB + \xi) \quad (11)$$

The plus sign is valid for n- and the minus sign for p-type material. Because for a p-type semiconductor, BB and ξ are negative, ϕ_b^B and ϕ_s^0 are always positive. Inserting eq 11 into eq 9, we get

$$\phi_b = \pm \gamma(CPD_L + \xi) \pm (1 - \gamma)(BB + \xi) \rightarrow$$
$$\phi_b \mp BB = \pm\gamma(CPD_L - BB) \pm \xi \quad (12)$$

Hence, a plot similar to Figure 7 but with correcting both sides for the measured BB should give a straight line with slope γ ($-\gamma$).

Making this correction, i.e., accounting for "free" surface states, does not improve significantly the correlations given in Table 2 for CPD_L vs barrier height plots, and more seriously, it cannot at all account for the negative γ we get (i.e., correcting for the band bending does not change the sign of γ). Therefore, the effect of the molecules on the barrier height cannot be ascribed to their interaction with the "free" surface states. In the next section we will show that the LUMO parameter can answer this riddle.

5.3.c. Molecular Dipole Effect on Barrier Height. The barrier height of the majority of the junctions showed the best correlation with the change in the molecules' LUMO energies. To understand how this correlation actually teaches us one of the fundamental effects that molecules can have on metal-semiconductor junction characteristics, we first consider shortly the relation between the different molecular properties and then explain how the sign of the slope of the molecular parameter vs barrier height plot inverts with the LUMO.

When considering the correlations given in Table 2, we should be aware of the fact that, by changing the substituent group, we alter simultaneously the molecular energy levels and the dipole moment (as well as other properties, e.g., hydrophobicity). Still, because we use a series of molecules rather than a single one, we can find the most relevant property. To show this, let us consider results obtained for junctions with a MoL of the nonsubstituted molecule (H). The dipole moment of that molecule (see Table 1) is close to that obtained with electron-withdrawing substituents (Me, OMe), but its LUMO value is more like that of the molecules with electron-donating groups (CN, CF_3). In addition the CF_3-substituted molecule has the highest dipole, but it has a LUMO value that is intermediate in the series of molecules used. Thus, the reason the CF_3 derivative's value in Figure 7 does not "fit" the general trend is simply because, though the surface CPD_L (*X*-axis) is related to the molecular dipole (see Figure 3), the barrier height (*Y*-axis) is influenced more by the molecule's LUMO than by its dipole.

Table 2 indeed shows that correlating the barrier height changes with those in dipole moment is equivalent to the CPD_L correlation but with opposite sign. This is so because $\chi^{eff} = \chi + \Delta\phi_{dip}$ and $Ip^{eff} = Ip + \Delta\phi_{dip}$, so that CPD_L will have a negative linear dependence on $\Delta\phi_{dip}$ (cf. eqs 1a,b) and, thus, on the molecular dipole, μ (cf. eq 8). The advantage of the CPD_L presentation is that it allows comparison of the molecular extent of the effect, even if the structural parameters of the molecular layers differ somewhat from one substituent to the other. This is so because there is no a priori reason, especially not with LOFO, for the molecular layers on the "free" surface and at the interface to differ significantly, as both are prepared under identical conditions. Hence the strength of the presentation of Figure 7 is that it compares two condensed molecular phases, whereas comparison of the molecular effect on the barrier height with any other molecular parameter requires use of values that are calculated/valid for isolated molecules.

5.3.d. LUMO and Molecular Electronegativity (Bond Polarization View). The clear LUMO effect can be understood by realizing that the LUMO energy reflects the electron affinity of the molecule.[90,91] This, in turn, can be related to the molecule's electronegativity (EN), which, in Mulliken's definition, is taken as the arithmetic mean of the electron affinity and the ionization potential,[92] i.e., EN = (LUMO + HOMO)/2.

We can, thus, relate the slope of the change in barrier height vs the molecular LUMO (cf. Figures 5 and 6) to the earlier mentioned *S* factor (the slope of a plot of barrier height vs metal electronegativity[52]). Table 2 shows that the *S* and γ factors we get have opposite signs and that inversion occurs between the first three junction types and the rest, as will be further discussed in section 5.4.a. The inversion between the *S* and γ factors is a result of our sign convention for CPD_L. In absolute terms, *S* values are smaller than γ ones. This is because γ scales between two condensed-phase properties (BH and CPD_L of the MoL on the surface), while *S* scales the BH (condensed phase) with the energy of an *isolated* molecule (gas phase). The latter is likely to be reduced upon formation of the 2-dimensional, condensed phase, MoL (e.g., by depolarization[81]).

The physical meaning of the electronegativity (or heat of formation[71,93,94]) as used for inorganic junctions is that it reflects polarization of interfacial bonds (resulting in interfacial dipoles). With the molecules the correlation factors shown in Table 2 suggest that the electron affinity ($\approx$LUMO[90,91]) might be a better measure for such interfacial polarization than EN. In any case the results show that such polarization can play a major role in dictating the net barrier height of the junctions, in contrast to the pure Schottky−Mott and Bardeen models, which are based on the macroscopic charge balance between either the bulk (Schottky−Mott) or the surface (Bardeen) electrochemical potential. This issue was recently reviewed by Tung.[31] He also pointed out the similarity between the bond-polarization and the so-called MIGS (metal-induced gap state) model (cf. also Chapter 6 in ref 49 for a short discussion). The effect of bond polarization can be illustrated by Figure 1. Inserting a layer of dipoles into the interface will modify the electrostatic potential difference across the interface, which will change the barrier height (cf. section 5.2 above). However, even if there are no molecules at the interface, the layer of dipoles of Figure 1d simply depicts the charge distribution of the interfacial bond. Such interface dipoles result from electronic interactions between the outermost atoms of the constituting phases. Hence, the electronegativity[52] (or bond polarization[31]) view can actually be put within the general Schottky−Mott model. It differs from the basic model in that the microscopic interfacial dipole contribution is added to the net potential balance.

How can we view such an interfacial dipole between a *metal* and molecule, where the dicarboxylic acid derivatives are chemically bound to the *GaAs* side? These molecules are closed-shell systems, and therefore it is unlikely that atoms of the metal will form strong chemical bonds with the molecule's substituents (which will be facing the metal). The soft deposition method we use also excludes the possibility of major damage to the molecule. It is indeed likely that top contact deposition via LOFO does not induce any structural or chemical changes in the molecular layer. This then suggests that the large barrier height modification dependence on the LUMO is due purely to rearrangement of the *charge* within the hybrid (molecule/metal) interface.[32,95]

5.4. Importance of the Microscopic Nature of the Junction for Molecular Effects. *5.4.a. Inversion Due to Pad Morphology.* The striking result of Figure 5 is the inversion of the molecular effect depending on the junction preparation mode. This is further revealed by the opposite signs of the γ and *S* factors, shown in Table 2.

We explain the inversion by suggesting a schematic description of the junction cross section as given in Figure 9. Experimentally, we observe drastic morphological differences between the metal pads, depending on whether they are put on the semiconductor surface by slow (Figure 9a) or normal (Figure

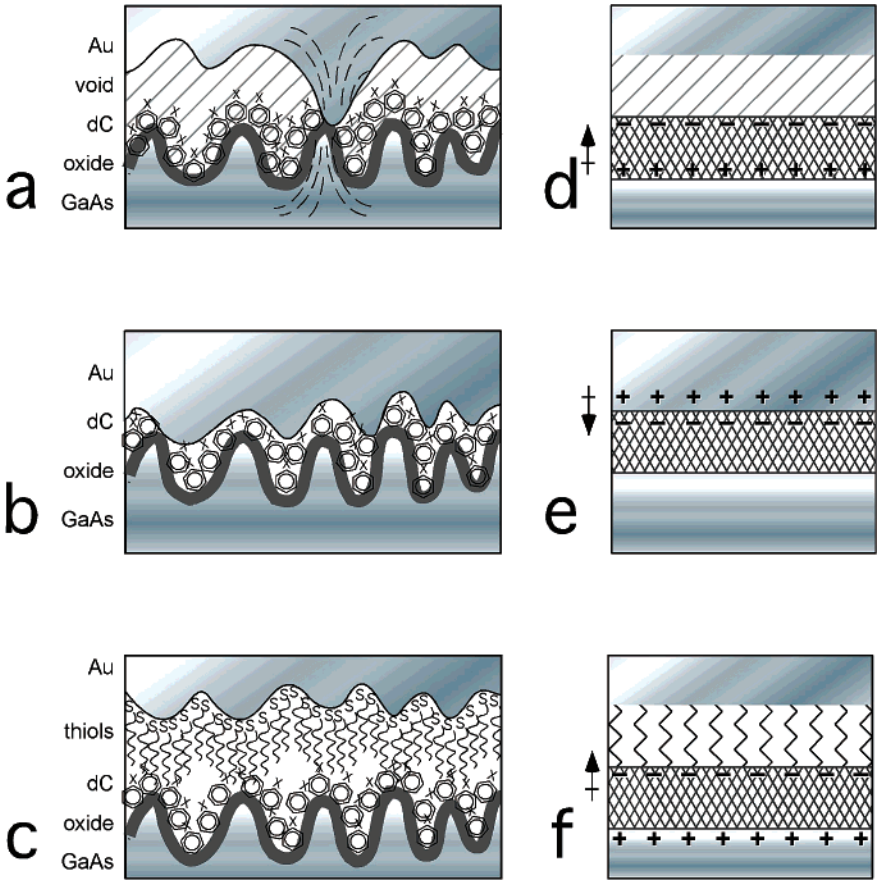

Figure 9. Schematic cross-section of a molecularly modified junction (left) and the resulting polarization (right). (a) Slow LOFO, characterized by "point" contacts via pinholes, to the metal, with high current density (dashed lines). (b) LOFO with atomic scale separation between the metal atoms and the MoL. (c) Double adsorption of a spacer MoL (zigzag) on the gold and dC (phenyls) on the GaAs. The surface roughness of both solids is assumed to be on the order of the dC thickness (∼1 nm) and the same thickness of oxide (dark line) exists on the GaAs side in all cases. The dC MoL has only average order (perpendicular to the surface). The right columns describe the suggested charge distribution for the case of an electron-withdrawing substituent on the molecule (e.g., CN, represented by X in (a)−(c); see also Table 1). Whenever the Au atoms are far away from the dC MoL (a, c) the molecular dipole is unchanged, and the extra charge on the substituent is withdrawn from the rest of the molecule, via the phenyl group, down to the binding group (CO_2−Ga^+). However, when there is intimate contact with the metal (b) the Au atoms are close enough to interact with the MoL and to alter the original molecular dipoles. Slow LOFO deposition (a) results in a pad roughness on the order of 100 nm.[59] Hence, only isolated points actually contact the GaAs, which results in a high series resistance due to spreading resistance. The interface charging is similar to that of the free surface because in most of the area the Au atoms are far (>10 nm) from the MoL. In contrast, after LOFO deposition (b) the substituted phenyl ring can interact strongly with the nearby Au atoms, changing the initial charge distribution (and dipole) of the isolated molecule.

9b) LOFO. Slow LOFO produces highly wrinkled pads with a roughness on the order of 100 nm compared to less than 10 nm for normal LOFO.[59] The electrical effect of the different roughness is clearly expressed in the series resistance, which is ∼200 times larger with the rough pad than with the smooth pad (Table 3). The high series resistance is readily explained by the spreading resistance of the tip-like contact points through which the current has to pass (dotted lines in Figure 9a). The ideality factors are also considerably higher, for junctions prepared by slow LOFO, than for those prepared by normal LOFO. Thus the indirect electrical parameters are clearly affected by the morphological change. We will argue here that also the charge distribution at the interface is dictated by the morphology.

On the right of Figure 9 we show the charge distribution for a molecular layer with an electron-withdrawing substituent group (e.g., CN) for different junction types. Evidence for the net (relative) dipole direction (sketched to the left of each panel) comes from the experimentally determined direction of the change in the barrier height. This direction depends on the nature of the molecules making up the layer (electron-withdrawing or electron-donating). For a rough pad (Figure 9a,d) the direction of change fits with the dipole direction of the free molecule and that found for the molecular film on a free surface. For smooth pads (Figure 9b,e) the change in barrier height is opposite to that expected from the dipole direction of free molecules, or surface-bound molecules. Therefore, in the cases shown in Figure 9d,f the poles of the dipole remain as in the free molecule, whereas for that shown in Figure 9e we assume that the molecule withdraws a net charge from the metal side (modifies the electron density spillover outside the metal surface), leaving behind an image charge as mentioned above (section 5.3.d).

The dependence of dipole direction on junction morphology indicates that it is the result of short-range interaction between the molecules and the metal. For the rough pad, the interactions are absent in most of the pad area. Even though it is likely that at the small contact area with the metal the dipole is altered, as argued above (section 5.2.b), the resulting net barrier will be dominated by the large area around the contact. Therefore, the net molecular effect on the barrier height is as if the molecular layer was not in contact.

To test this assumption, we modified the Au pad in such a way so as to insert a narrow dielectric layer between the metal and the active molecules. The results are those obtained for the

junction type named "thiols" (SC_{12}) in the Results. This junction is identical to the previous ones on the GaAs side, but with a layer of supposedly electrically insulating C_{12} alkanethiols ($\sim$1 nm thick) adsorbed on the gold side. The resulting pads were as smooth as those obtained with nonmodified Au[59] (Figure 9b). Still, from Figure 5 and Table 2 we see that, electrically, the double adsorbed junctions (Figure 9c) behave like the rough pads (Figure 9a) with a molecular effect that is even somewhat stronger than that obtained for singly adsorbed, slow LOFO-prepared junctions.

This analysis explains the inversion in γ and S factors. For the spaced junctions the metal and the molecules do not interact chemically (or in any other quantum mechanical fashion); hence, the relevant interface factor is γ, accounting for the characteristics of the *surface*. If, however, the metal and molecular group can interact (i.e., significant overlap of their wave functions), then S becomes the relevant parameter and accounts for the extent of interactions at the *interface formed* between the two constituent surfaces. This argument is supported by comparing the slow LOFO- and normal LOFO-prepared junctions. With the former the correlation with CPD_L was much better than with LUMO or EN, whereas the opposite holds for the latter.

5.4.b. Comparing LOFO and Evaporation. Interestingly, the structural influence was evident also *in those cases where top contacts could be evaporated on a series of molecules* (without damaging them; see section 4.3 and Figure 6). Looking at the barrier height data obtained by evaporation at low base pressure, we see a behavior that is almost identical to that obtained with normal LOFO. If we now introduce Ar into the chamber to produce milder evaporation conditions, we find the opposite molecular effect. For this junction the molecular effect was also the smallest, almost in the range of the error bars (Figure 6). This suggests that this type of evaporation leaves a residual layer between the MoL and the metal, which suffices to buffer the short-range charging.

Thus the evaporation results generally support our conclusion that LOFO yields very "intimate" junctions, with a negligible residual layer between the contacting phases. However, the bare junctions that were prepared by evaporation showed a large difference with the LOFO-prepared ones as well as with those with a MoL.[59] This agrees with other results of ours[96−98] that the dC molecules stabilize the surface chemically. As our main interest was in the LOFO procedure, we did not further characterize the evaporated junctions. Even so, our results show (again) that metal evaporation onto molecules is not trivial, and special attention should be paid to the interfacial chemistry (cf., for example, ref 58). In our case we can achieve better control over the resulting junctions with the LOFO procedure than with evaporation. Still, this should not be viewed as a fundamental difference between the methods, as can be seen from the very similar results we get for Au/n-GaAs junctions made by LOFO (Figure 5) and one case of evaporation under high vacuum (Figure 6).

5.4.c. Differences between p- and n-GaAs. The last major finding we report here is that changing the majority charge carriers from electrons to holes drastically increases the effect of the same set of dicarboxylic derivatives, as can be seen from Table 2 (BH span). Qualitatively, we can say that the larger effect on p-type results from the (Lewis) acidic nature of the molecules that behave as acceptors. A high density of interface acceptors will reduce the barrier on p-type junctions but should increase it for an n-type material. Studies of the effects of adatoms on semiconductor surfaces showed that, all other factors being equal, a given surface band bending is more readily decreased than increased.[99] Therefore, assuming that, because of their acceptor character, the molecules will localize negative charge on the semiconductor surface, it will be more difficult to increase the barrier with n-type material than to decrease it for p-type. The same argument can also explain the larger dC effect on the free surface band bending of p- vs n-GaAs.

This doping dependence can also be understood by the general nature of the barrier as an averaged property. Vittoro et al.[77] showed that the lower the work function of the metal (for n-GaAs) the more sensitive the barrier is toward interface states. In this regard we can view the molecular effect on the barrier as a perturbation on the clean interface barrier.[77] Similarly, the smaller the barrier of the junction without a MoL, the stronger will be the effect of the MoL that we can expect. The smallest difference in work functions is between Au and p-GaAs (compared to both Al/p-GaAs or Au/n-GaAs) and, therefore, the Au/p-GaAs system gives the largest molecular expression.

Another limitation that we should consider is the effect of defects. Because the current depends exponentially on the barrier, low-barrier defects have a much larger effect than their nominal area.[86,87] In contrast, high barrier defects will have practically no effect. Therefore, an interfacial dipole that reduces the barrier will be expressed strongly, whereas the effect of an opposite dipole will be screened by defects with barriers lower than the surrounding. In other words, it is much easier to reduce the barrier than to increase it. This can explain the fact that the molecules generally reduce the barrier, simply because the opposite effect is truncated. The same argument also explains the much larger MoL effect on the BH of junctions with p-type than with n-type junctions. If we assume that the net (negative) charging of dC−CN is larger than the (positive) charging of dC−OMe ligands, the large effect of the CN will be expressed fully with p-type material, but will be damped for the n-type junction. The reason is that in the p-type junction it acts to reduce the barrier, whereas in the n-type material it cannot increase the barrier significantly above that dictated by the defects. As a result of this, when we sum the barrier heights to p- and n-type material for a given substituent (cf. eq 7 and Figure 8), the opposite contributions are not balanced and the sum is less than expected (Figure 8). The dC−OMe-based ligands should be most effective in reducing the barrier for n-type, but the initial driving force in this case is smaller. Therefore, the n- and p-type contributions of dC−OMe are balanced, as expressed in Figure 8 (the positive difference is due to other effects, as described in section 5.1.c).

5.4.d. Major Considerations To Enhance Molecular Expression. Last, we present the major practical considerations for choosing molecules to modify the barrier height of a given interface:

- It is always easier to reduce a barrier than to increase it.
- The molecular expression increases as the background barrier decreases.
- It is easier to place a negative charge on the dC skeleton than a positive one. In general, the net charging of the molecule will probably depend on the binding group, an issue that we are currently studying.[100]
- Metal/organic charging can be blocked by a thin insulating layer. In such a case the native charge distribution of the molecule controls the barrier.[44]

6. Summary

We have studied the effect on the barrier height of insertion of a 1 nm thick molecular layer into a solid, inorganic interface. The molecular characteristics are not screened by the electrically

dense metal; on the contrary, they modify the properties of the solid interface. Yet close proximity of the metal to the molecules can charge the molecular layer even without covalent binding. Such charging can be blocked by a thin (∼1 nm) buffer layer. Charge rearrangement across the contact must be taken into consideration when molecule/metal junctions are designed, either macro- or microscopic, as it is expected to highly modify the net effect of the molecules. The ability of a thin organic layer to accommodate charge appears, at present, to be an aspect of the study of molecules for electronics that is not so much appreciated. Modeling of this (static) charge transfer relates to fundamental questions regarding the interactions between localized (molecular) and extended (solid) energy levels. It would appear to be important for any system where molecules are coupled to electronic materials. A major advantage of the static charging approach to molecule-based devices, over the dynamic one, where charge has to pass through molecules, is that it can tolerate low perfection in the MoL. It could have practical implications for biosensors, and for achieving better control over band alignment at organic/metal interfaces.

Acknowledgment. We are grateful to Prof. A. Shanzer and Ms. Rachel Lazar (all from the Org. Chem. Department, WIS) for synthesis of the organic molecules. We, and especially J.G., thank Prof. G. J. M. Martin for his guidance and advice with the quantum chemical calculations. We thank the Israel Science Foundation, Jerusalem, and the Israel Ministry of Science (Tashtyoth program) for financial support.

Supporting Information Available: Ellipsometry data and their discussion are available free of charge via the Internet at http://pubs.acs.org.

References and Notes

(1) Miles, J. L.; McMahon, H. O. *J. Appl. Phys.* **1961**, *32*, 1176.
(2) Joachim, C.; Gimzewski, J. K.; Aviram, A. *Nature* **2000**, *408*, 541.
(3) Petty, M. C.; Bryce, M. R.; Bloor, D. *An Introduction to Molecular Electronics*, 1st ed.; Edward Arnold: London, 1995.
(4) Richardson, T. Langmuir−Blodgett films. In *An Introduction to Molecular Electronics*, 1st ed.; Petty, M. C., Bryce, M. R., Bloor, D., Eds.; Edward Arnold: London, 1995; Chapter 10, p 220.
(5) Mann, B.; Kuhn, H. *J. Appl. Phys.* **1971**, *42*, 4398.
(6) Honig, E. P. *Thin Solid Films* **1976**, *33*, 231.
(7) Polymeropoulos, E. E. *J. Appl. Phys.* **1977**, *48*, 2404.
(8) Polymeropoulos, E. E.; Sagiv, J. *J. Chem. Phys.* **1978**, *69*, 1836.
(9) Tredgold, R.; Vickers, A.; Allen, R. *J. Phys. D* **1984**, *17*, L5.
(10) Race, H. H.; Reynolds, S. I. *J. Am. Chem. Soc.* **1939**, *61*, 1425.
(11) Itoh, E.; Iwamoto, M. *J. Appl. Phys.* **1999**, *85*, 7239.
(12) Slowinski, K.; Fong, H. K. Y.; Majda, M. *J. Am. Chem. Soc.* **1999**, *121*, 7257.
(13) Holmlin, R. E.; Ismagilov, R. F.; Haag, R.; Mujica, V.; Ratner, M. A.; Rampi, M. A.; Whitesides, G. M. *Angew. Chem., Int. Ed.* **2001**, *40*, 2316.
(14) Selzer, Y.; Cahen, D. *Adv. Mater.* **2001**, *13*, 508.
(15) Selzer, Y.; Salomon, A.; Cahen, D. *J. Am. Chem. Soc.* **2002**, *124*, 2886. *J. Phys. Chem. B* **2002**, *106*, 10432.
(16) Roth, S.; Burghard, M.; Fischer, C. M. Resonant tunneling and molecular rectification in Langmuir−Blodgett films. In *Molecular electronics*; Jortner, J., Ratner, M., Eds.; Blackwell Science: Oxford, U.K., 1997; p 255.
(17) Wong, E. W.; Collier, C. P.; Behloradsky, M.; Raymo, F. M.; Stoddart, J. F.; Heath, J. R. *J. Am. Chem. Soc.* **2000**, *122*, 5831.
(18) Collier, C. P.; Mattersteig, G.; Wong, E. W.; Luo, Y.; Beverly, K.; Sampaio, J.; Raymo, F. M.; Stoddart, J. F.; Heath, J. R. *Science* **2000**, *289*, 1172.
(19) Evans, S. D.; Ulman, A. *Chem. Phys. Lett.* **1990**, *170*, 462.
(20) Evans, S. D.; Urankar, E.; Ulman, A.; Ferris, N. *J. Am. Chem. Soc.* **1991**, *113*, 4121.
(21) Seker, S.; Meeker, K.; Keuch, T. F.; Ellis, A. B. *Chem. Rev.* **2000**, *100*, 2505.
(22) We use the term molecular layer (MoL) instead of monolayer (ML), to stress the difference between these layers, on the one hand, and near-perfectly ordered monolayers with both local and long-range order, on the other hand. In our case, there is average order, perpendicular to the binding surface, because we use ligands with a well-defined binding site. We followed adsorption procedures to avoid multilayers on the surface. Total coverage can vary from 0.75 to 1 monolayer, depending on the binding groups, substituents, and substrate.
(23) Bruening, M.; Moons, E.; Yaron-Marcovich, D.; Cahen, D.; Libman, J.; Shanzer, A. *J. Am. Chem. Soc.* **1994**, *116*, 2972.
(24) Vilan, A.; Cahen, D. *Trends Biotechnol* **2002**, *20*, 22.
(25) Ashkenasy, G.; Cahen, D.; Cohen, R.; Shanzer, A.; Vilan, A. *Acc. Chem. Res.* **2002**, *35*, 121.
(26) Cohen, R.; Kronik, L.; Vilan, A.; Shanzer, A.; Cahen, D. *Adv. Mater.* **2000**, *12*, 33.
(27) Carrara, M.; Nuesch, F.; Zuppiroli, L. *Synth. Met.* **2001**, *121*, 1633.
(28) Winter, C.; Tredgold, R.; Hodge, P.; Khoshdel, E. *IEE Proc. Pt. I* **1984**, *131*, 125.
(29) Tredgold, R.; Badawy, Z. E. *J. Phys. D* **1985**, *18*, 2483.
(30) Tredgold, R.; Badawy, Z. E. *J. Phys. D* **1985**, *18*, 103.
(31) Tung, R. T. *Mater. Sci. Eng. R* **2001**, *35*, 1.
(32) Ishii, H.; Sugiyama, K.; Ito, E.; Seki, K. *Adv. Mater.* **1999**, *11*, 605.
(33) Hill, I. G.; Rajagopal, A.; Kahn, A. *J. Appl. Phys.* **1998**, *84*, 3236.
(34) Schlettwein, D.; Hesse, K.; Gruhn, N. E.; Lee, P. A.; Nebesny, K. W.; Armstrong, N. R. *J. Phys. Chem. B* **2001**, *105*, 4791.
(35) Campbell, L. H.; Kress, J. D.; Martin, R. L.; Smith, D. L.; Barashkov, N. N.; Ferraris, J. P. *Appl. Phys. Lett.* **1997**, *71*, 3528.
(36) Campbell, L. H.; Rubin, S.; Zawodzinski, T. A.; Kress, J. D.; Martin, R. L.; Smith, D. L.; Barashkov, N. N.; Ferraris, J. P. *Phys. Rev. B* **1996**, *54*, 14321.
(37) Nuesch, F.; Rotzinger, F.; Si-Ahmed, L.; Zuppiroli, L. *Chem. Phys. Lett.* **1998**, *288*, 861.
(38) Zuppiroli, L.; Si-Ahmed, L.; Kamaras, K.; Nuesch, F.; Bussac, M.; Ades, D.; Siove, A.; Moons, E.; Gratzel, M. *Eur. Phys. J. B* **1999**, *11*, 505.
(39) Gal, D.; Sone, E.; Cohen, R.; Hodes, G.; Libman, J.; Shanzer, A.; Schock, H. W.; Cahen, D. *Proc. Ind. Acad. Sci. Chem. Sci.* **1997**, *109*, 487.
(40) Krüger, J.; Bach, U.; Grätzel, M. *Adv. Mater.* **2000**, *12*, 447.
(41) Ganzorig, C.; Kwak, K. J.; Yagi, K.; Fujihira, M. *Appl. Phys. Lett.* **2001**, *79*, 272.
(42) Nuesch, F.; Forsythe, E. W.; Le, Q. T.; Gao, Y.; Rothberg, L. J. *J. Appl. Phys.* **2000**, *87*, 7973.
(43) Salomon, A.; Berkovich, D.; Cahen, D. *Appl. Phys. Lett.* **2003**, *82*.
(44) Vilan, A.; Shanzer, A.; Cahen, D. *Nature* **2000**, *404*, 166.
(45) Wu, D. G.; Ghabboun, J.; Martin, J. M. L.; Cahen, D. *J. Phys. Chem. B* **2001**, *105*, 12011.
(46) Bonifazi, D.; Salomon, A.; Enger, O.; Diederich, F.; Cahen, D. *Adv. Mater.* **2002**, *14*, 802.
(47) Brillson, L. J. *Contacts to semiconductors*; *Fundamentals and technology*; Noyes: NJ, 1993.
(48) Lüth, H. *Surfaces and Interfaces of Solid Materials*, 3rd ed.; Springer-Verlag: Berlin, 1998.
(49) Mönch, W. *Semiconductors surfaces and interfaces*, 2nd ed.; Springer: Berlin, 1995.
(50) Sze, S. M. *Physics of Semiconductor Devices*, 2nd ed.; Wiley: New York, 1981.
(51) Cowley, A. M.; Sze, S. M. *J. Appl. Phys.* **1965**, *36*, 3212.
(52) Kurtin, S.; McGill, T. C.; Mead, C. A. *Phys. Rev. Lett.* **1970**, *22*, 1433.
(53) Cohen, R.; Kronik, L.; Shanzer, A.; Cahen, D.; Liu, A.; Rosenwaks, Y.; Lorenz, J.; Ellis, A. B. *J. Am. Chem. Soc.* **1999**, *121*, 10545.
(54) Bastide, S.; Butruille, R.; Cahen, D.; Dutta, A.; Libman, J.; Shanzer, A.; Sun, L.; Vilan, A. *J. Phys. Chem.* **1997**, *101*, 2678.
(55) Vilan, A.; Ussyshkin, R.; Gartsman, K.; Cahen, D.; Naaman, R.; Shanzer, A. *J. Phys. Chem.* **1998**, *102*, 3307.
(56) The different adsorption conditions required for the methoxy (OMe) termination are probably due to the resulting high concentration of negative charge on the binding end, making the radical or the carboxylate form energetically unfavorable. We suggest that the added water stabilizes these species, hence allowing their adsorption. We note that adding water is not always beneficial for adsorption. Thus, for example, addition of a few % (v/v) H_2O to the acetonitrile solution will precipitate the nonsubstituted (H) dC ligands as a thick layer on the surface.
(57) Ulman, A. *An Introduction to Ultrathin Organic Films*; Academic Press: New York, 1991.
(58) Hooper, A.; Fisher, G. L.; Konstadinidis, K.; Jung, D.; Nguyen, H.; Opila, R.; Collins, R. W.; Winograd, N.; Allara, D. L. *J. Am. Chem. Soc.* **1999**, *121*, 8052.
(59) Vilan, A.; Cahen, D. *Adv. Funct. Mater.* **2002**, *12*, 795.
(60) Pople, J. A. *Angew. Chem., Int. Ed.* **1999**, *38*, 1894.
(61) Selzer, Y.; Salomon, A.; Ghabboun, J.; Cahen, D. *Angew. Chem., Int. Ed.* **2002**, *41*, 827.
(62) Frisch, M. J.; Trucks, G. W.; Schlegel, H. B.; Scuseria, G. E.; Robb, M. A.; Cheeseman, J. R.; Zakrzewski, V. G.; Montgomery, J. A.; Stratmann,

R. E.; Burant, J. C.; Dapprich, S.; Millam, J. M.; Daniels, A. D.; Kudin, K. N.; Strain, M. C.; Farkas, O.; Tomasi, J.; Barone, V.; Cossi, M.; Cammi, R.; Mennucci, B.; Pomelli, C.; Adamo, C.; Clifford, S.; Ochterski, J.; Petersson, G. A.; Ayala, P. Y.; Cui, Q.; Morokuma, K.; Malick, D. K.; Rabuck, A. D.; Raghavachari, K.; Foresman, J. B.; Cioslowski, J.; Ortiz, J. V.; Baboul, A. G.; Stefanov, B. B.; Liu, G.; Liashenko, A.; Piskorz, P.; Komaromi, I.; Gomperts, R.; Martin, R. L.; Fox, D.; Keith, T.; Al-Laham, M. A.; Peng, C. Y.; Nanayakkara, A.; Gonzalez, C.; Challacombe, M.; Gill, P. M. W.; Johnson, B.; Chen, W.; Wong, M. W.; Andres, J. L.; Gonzalez, C.; Head-Gordon, M.; Replogle, E. S.; Pople, J. A. *Gaussian 98*, revision A.7 ed.; Gaussian, Inc: Pittsburgh, PA, 1998.

(63) Stewart, J. P. *J. Comput. Chem.* **1989**, *10*, 221.

(64) Becke, A. D. J. *J. Chem. Phys.* **1993**, *98*, 5648.

(65) Dunning, T. H., Jr. *J. Chem. Phys.* **1989**, *90*, 1007.

(66) Kronik, L.; Shapira, Y. *Surf. Sci. Rep.* **1999**, *37*, 1.

(67) 1D = 3.336 $\times 10^{-30}$ C·m, which is the MKS unit for the dipole moment.

(68) XPS confirmed the presence and the stoichiometry of the adsorbed molecules with their substituent elements (e.g., N, F) at their outside, on top of an oxide layer composed of Ga and As in lower (than III) oxidation state. The thickness extracted based on different elements varies slightly and was 10 ± 4 Å for both the MoL and the oxide, in agreement with our ellipsometry data (cf. supplementary information).

(69) Rhoderick, E. A.; Williams, R. H. *Metal-semiconductor contacts*, 2nd ed.; Clarendon: Oxford, U.K., 1988.

(70) Supply and other technical problems prevented us from collecting the complete series of data, including the OMe derivative, for vacuum evaporation without Ar.

(71) Brillson, L. J. *Surf. Sci. Rep.* **1982**, *2*, 123.

(72) Waldrop, J. R. *Appl. Phys. Lett.* **1988**, *53*, 1518.

(73) Werner, J. H. *Appl. Phys. A* **1988**, *47*, 291.

(74) Vilan, A.; Cahen, D., in preparation.

(75) Myburg, G.; Auret, F. D.; Meyer, W. E.; Louw, C. W.; van Staden, M. J. *Thin Solid Films* **1998**, *325*, 181.

(76) Chang, S.; Raisanen, A.; Brillson, L. J.; Shaw, J. L.; Kirchner, P. D.; Pettit, G. D.; Woodall, J. M. *J. Vac. Sci. Technol. B* **1992**, *10*, 1932.

(77) Viturro, R. E.; Chang, J. L.; Shaw, J. L.; Mailhiot, C.; Brillson, L. J. *J. Vac. Sci. Technol. B* **1989**, *7*, 1007.

(78) Chang, S.; Brillson, L. J.; Kime, Y. J.; Rioux, D. S.; Kirchner, P. D.; Pettit, G. D.; Woodall, J. M. *Phys. Rev. Lett.* **1990**, *64*, 2551.

(79) Estimates of the contact area, independent of the barrier height can be gotten by measuring the $I-V$ characteristics as a function of temperature, or use of additional methods such as capacitance−voltage and internal photoemission measurements. We have experimented with both temperature-dependent $I-V$ and capacitance−voltage measurements and find their interpretation to be even less straightforward than that of the current−voltage ones. Thus, though definitely worthwhile, they will require a major further effort to bear fruit.

(80) Dharmadasa, I. M.; Roberts, G. G.; Petty, M. C. *Electron. Lett.* **1980**, *16*, 201.

(81) Iwamoto, M.; Mizutani, Y.; Sugimura, A. *Phys. Rev. B* **1996**, *54*, 8186.

(82) Bruening, M.; Cohen, R.; Guillemoles, J. F.; Moav, T.; Libman, J.; Shanzer, A.; Cahen, D. *J. Am. Chem. Soc.* **1997**, *119*, 5720.

(83) van Ruyven, L. J. *Phys. Stat. Solidi* **1964**, *5*, K109.

(84) dell'Orto, T.; Almeida, J.; Coluzza, C.; Baldereschi, A.; Maragaritondo, G.; Cantile, M.; Yildirim, S.; Sorba, L.; Franciosi, A. *Appl. Phys. Lett.* **1994**, *64*, 2111.

(85) Franciosi, A.; Van de Walle, C. G. *Surf. Sci. Rep.* **1996**, *25*, 1.

(86) Tung, R. T. *Phys. Rev. B* **1992**, *45*, 13509.

(87) Werner, J. H.; Guttler, H. H. *J. Appl. Phys.* **1991**, *69*, 1522.

(88) The slope values were extracted by us from the experimental data of Myburg et al.[75]

(89) This procedure was found to give cleaner and smoother surfaces under nonclean room conditions.

(90) We take the energy difference between the neutral molecule and the radical anion, formed by adding an electron to it, as the electron affinity of a molecule. In calculations relaxation effects are neglected and the calculations are for the geometry of the neutral species; cf. also Vondrak et al.[91]

(91) Vondrak, T.; Cramer, C. J.; Zhu, X. Y. *J. Phys. Chem. B* **1999**, *103*, 8915.

(92) Huheey, J. E. *Inorganic Chemistry*, 3rd ed.; Harper: New York, 1983.

(93) This connection is understandable from Pauling's original definition of electronegativity, which involved bond dissociation energies (cf. Huheey[92]), and from Miedema's work on alloys (Miedema et al.[94]).

(94) Miedema, A. R.; De Boer, F. R.; De Chatel, P. F. *J. Phys. F* **1973**, *3*, 1558.

(95) Blyth, R. I. R.; Mittendorfer, F.; Hafner, J. H.; Sardar, S. A.; Duschek, R.; Netzer, F. P.; Ramsey, M. G. *J. Chem. Phys.* **2001**, *114*, 935.

(96) Wu, D. G.; Ashkenasy, G.; Shvarts, D.; Ussyshkin, R. V.; Naaman, R.; Shanzer, A.; Cahen, D. *Angew. Chem., Int. Ed.* **2000**, *39*, 4496.

(97) Wu, D.; Cahen, D.; Graf, P.; R. Naaman, R.; Nitzan, A.; Shvarts, D. *Chem., Eur. J.* **2001**, *7*, 1743.

(98) Gartsman, K.; Cahen, D.; Kadyshevitch, A.; Libman, J.; Moav, T.; Naaman, R.; Shanzer, A.; Umansky, V.; Vilan, A. *Chem. Phys. Lett.* **1997**, *283*, 301.

(99) De Renzi, V.; Biagi, R.; del Pennino, U.; Pedio, M.; Goldoni, A.; Larciprete, R. *Phys. Rev. B* **2000**, *62*, R10657.

(100) Cahen, D.; Hodes, G. *Adv. Mater.* **2002**, *11*, 789.